

# Using Simulation at RF

By Dr. Ulrich Rohde, NIUL

## Introduction

While RF is ill-defined, RF effects start already at about 100 kHz. This was first noticed while building high Q inductors for receivers. At this time Litz wire was invented. Here braided copper wire was covered with cotton and these were braided again. So self-resonance effects were largely avoided.

The simulator, having a graphic input (schematic entry) and graphic output (rectangular or polar > Smith Chart) solves the DC/RF current calculation in the circuit based on the Z or Y matrix (Series or parallel circuits parts) based on the voltages applied. For passive components there are practically no distortion products and the calculations are trivial. As frequencies get higher, the physical dimensions will get closer to the wavelength and the RF values of the components change drastically. Even below these frequencies the passive elements will show the effects of parasitic elements such as lead inductors and stray capacitances.

To complicate matters active elements such as diodes and transistors force the designer to more complex simulators. Simulators should provide information about all practical circuits, from a low number of transistors to millions of them in ICs. Typical parameters are gain, input/output impedance or matching (S-parameters, noise figure and stability). Of course DC information is also available. For this purpose SPICE was developed. There are many dialects of SPICE available. From Cadence, SPECTRE is probably the most powerful on the market.

SPICE, while doing DC, frequency and time domain simulations, has some problems. The time domain calculation uses very complex mathematics. The algorithmic research carried out converged to the use of the Newton-Raphson solution on nonlinear equations. More detail is available from [11]. These methods are not always stable. All kind of experiments with the program settings may be necessary to get a conversion of the process; also SPICE has problems with very high-Q circuits. The noise analysis, if not based on the noise correlation matrix approach, is also not correct as the feedback capacitance  $\text{Im}(Y_{12})$  begins to play a key role. All modern SPICE programs are at least based on SPICE3 from Berkley.

The real powerful simulators however are based on the harmonic balance method where passive component circuit parts are calculated in the frequency domain and the nonlinear (active) components in the time domain.

This partly stems from the fact that the transient and time domain analysis is proportional to the values of the components. Therefore a 10nF capacitor requires more computation time as a 1nF capacitor. This is not the case in the frequency domain.

Generally, SPICE finds a solution to most circuit problems. However, because of the nonlinearity of the circuit equations and a few imperfections in the analytical device models a solution is not always guaranteed when the circuit and its specification are otherwise correct.

In the majority of the cases when a solution failure occurs it is due to a circuit problem, either its specification or its inoperability. A convergence problem can be categorized as either failure to compute a DC operating point or

abortion of the transient analysis because of the reduction for the time step below a certain limit without finding a solution.

Failure to find a solution can occur at the level of the linear equation, the Newton-Raphson iteration, or the numerical integration. Rather than present the convergence issues based on the algorithm causing the problem, it has been deemed beneficial to describe the causes for failure from a user's perspective.

Specific procedures can be followed when SPICE fails to find a DC solution of the circuit. The prescribed remedies include redefinition of analysis options, use of built-in convergence-enhancing algorithms, and DC operating point solution with a different analysis.

Time-domain analysis can provide an inaccurate solution or fail because of a number of reasons related either to the integration method and associated time-step control or the iterative solution of nonlinear equations. Knowledge of the specifics of different types of electronic circuits can assist the user in finding an accurate solution by specifying appropriate analysis modes, options, tolerances, and suitable model parameters. Thus, oscillators require certain initializations not necessary for amplifiers, and bipolar circuits may need different convergence tolerances than do MOS circuits. Also only the hybrid programs, based on SPICE type approach and harmonic balance and its dialects offer linear and non-linear optimization!

## 1. LIMITS OF LOW-FREQUENCY SIMULATION

### 1.1 Upper limit of conventional SPICE simulators

The basic SPICE simulator has ideal elements and some transmission line applications. As we approach frequencies where the lumped elements turn into distributed elements and special connecting elements become necessary, the use of the standard elements ends. It also has the mathematical limitations mentioned above. Temperature effects are allowed, meaning that the influence of temperature on the components is taken into account.

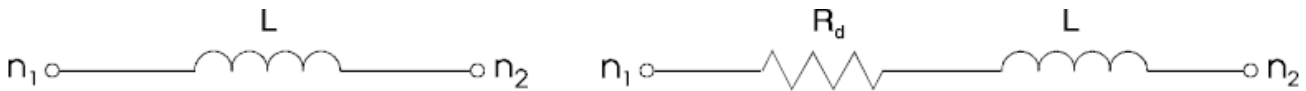
Here is a list of some standard passive devices and its description for temperature and frequency, which low frequency simulators don't have:

#### IND – Inductor [5]

Inductor has the following options:

- Ideal Inductor
- Toroidal Inductor
- Air Core Inductor

#### Ideal Inductor



keyword	description	unit	default
<b>L</b>	Inductance		
<b>Rs</b>	Series resistance		
<b>Q</b>	Quality factor, constant resistance with $Q$ specified		
<b>Q1</b>	Quality factor, resistance proportional to square root of frequency (skin-effect model)		
<b>Q2</b>	Quality factor, constant $Q$ model (resistance inversely proportional to frequency)		
<b>F</b>	Frequency at which quality factor ( <b>Q</b> , <b>Q1</b> or <b>Q2</b> ) has assigned value		
<b>TEMP</b>	Local temperature used for noise calculations	K	298
<b>TC1</b>	Temperature coefficient /degree		0.0
<b>TC2</b>	Temperature coefficient /degree2		0.0
<b>M</b>	Multiplication factor		1.0
<b>DTEMP</b>	Temperature difference	degree	0.0

#### Notes

1. The model is described by the following:

$$Q = \omega L / R_d$$

where  $\omega = 2\pi f$

$f$  = operating frequency

2. If **Rs** is specified,  $R_d = R_s$ .

3. If neither **Rs**, **Q**, **Q1**, nor **Q2** is specified, the inductor is assumed to be ideal; that is,  $R_d = 0$ .

4. Let  $Q_{REF}$ ,  $Q1_{REF}$  and  $Q2_{REF}$  represent the numeric values of  $Q$ ,  $Q1$  and  $Q2$ ; that is, the actual numbers that replace the symbol  $x2$ . Let  $F_{REF}$  represent the numeric value of  $F$ . The frequency dependence of the three  $Q$  models is given by

$$Q: Q(f) = Q_{REF} / F_{REF}$$

$$Q1: Q(f) = Q1_{REF} * \sqrt{\frac{f}{F_{REF}}}$$

$$Q2: Q(f) = Q2_{REF}$$

5. If an ideal inductor is referenced by the KMUI element, this inductor must be labeled.

Please see the reference for the KMUI element. The Label name can be entered through the element properties dialog.

6. If  $TC1$ ,  $TC2$ ,  $M$ , or  $DTEMP$  is defined, the inductance  $L$  represented by the IND element is given by

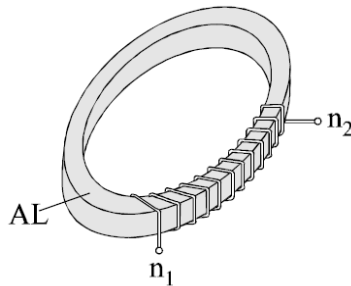
$$L = L * (1.0 + TC1 * DTEMP + TC2 * DTEMP^2) / M$$

### Toroidal Inductor

The Toroidal Inductor has the following options

- Ideal Model
- Physical Model

#### Ideal Inductor



#### keyword

**N**  
**AL**

#### description

Number of winding  
Inductance index

#### unit

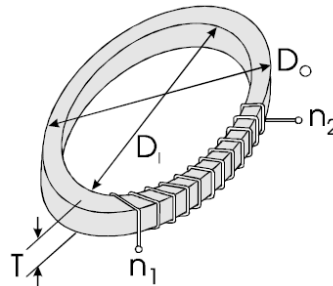
turns  
Henrys/turn

#### default

*Note*

$$L = N^2 * AL$$

#### PHYSICAL MODEL



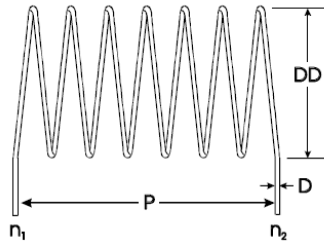
keyword	description	unit	default
DO	Outer diameter of core	meter	
DI	Inner diameter of core	meter	
N	Number of winding	turns	
T	Thickness of the core	meter	
MU	Relative permeability of the core		
RB	Conductor resistivity	micro-ohm*cm	0.0
D	Diameter of the wire	meter	0.0

### Air Core Inductor

The Air Core Inductor has the following options:

- Physical Model with wire diameter
- Physical Model with wire gauge

#### PHYSICAL MODEL WIRE DIAMETER [6]

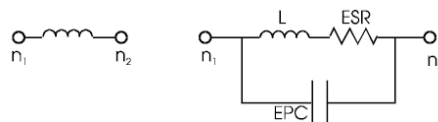


keyword	description	unit	default
DD	Diameter of the core	meter	
N	Number of winding	turns	
P	Physical length		
D	Diameter of the wire	meter	
RB	Conductor resistivity	micro-ohm*cm	

#### PHYSICAL MODEL WITH WIRE GAUGE

keyword	description	unit	default
DD	Diameter of the core	meter	
N	Number of winding	turns	
P	Physical length	meter	
AWG	Gauge of the wire		
RB	Conductor resistivity	micro-ohm*cm	

### INDQ – Chip Inductor 2



Keyword	description	unit	default
L	Inductance	Henry	0.0
FRES	Self-resonance frequency	Hz	0.0

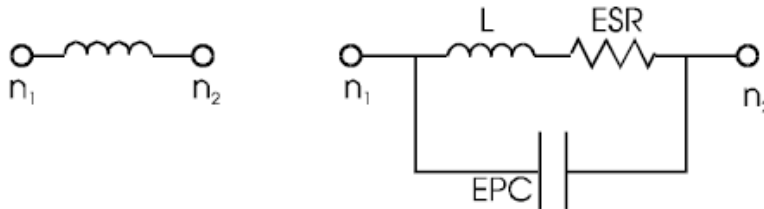
<b>Q</b>	Quality factor	0.0	
<b>FQ</b>	Frequency at which <b>Q</b> is given	Hz	0.0
<b>TC</b>	Temperature coefficient	PPM	0.0
<b>TEMP</b>	Element temperature	K	298
<b>MOD</b>	Keyword to indicate the name of a chip inductor in a related device library		

Notes

1. ESR is the equivalent series resistance and can be calculated from **Q** as  $ESR = 1/(\omega L \times Q)$ .
2. EPC is the equivalent parallel capacitance and can be calculated from the self-resonance frequency, **FRES**.
3. **TC** is defined in PPM (parts per million). For example, an inductor has a nominal value,  $L_0$  (keyword **L**), at 298 K. At temperature **TEMP**, the value  $L$  of the inductor is calculated as  

$$L = L_0 \times (1 + (\text{TEMP} - 298) \times \text{TC} \times 1.0e-6)$$

**INDR – Chip Inductor 3**



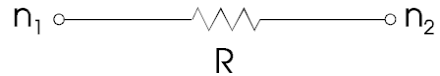
Keyword	Description	unit	default
<b>L</b>	Inductance	Henry	0.0
<b>FRES</b>	Self-resonance frequency	Hz	0.0
<b>ESR</b>	Equivalent series resistance	Ohm	0.0
<b>FESR</b>	Frequency at which ESR is given	Hz	0.0
<b>TC</b>	Temperature coefficient	PPM	0.0
<b>TEMP</b>	Element temperature	K	298
<b>MOD</b>	Keyword to indicate the name of a chip inductor in a related device library		

Notes

1. EPC is the equivalent parallel capacitance and can be calculated from the self-resonance frequency, **FRES**.
2. **TC** is defined in PPM (parts per million). For example, an inductor has a nominal value,  $L_0$  (keyword **L**) at 298 K. At temperature **TEMP**, the value of the inductor is calculated as  

$$L = L_0 \times (1 + (\text{TEMP} - 298) \times \text{TC} \times 1.0e-6)$$

## RES – Resistor



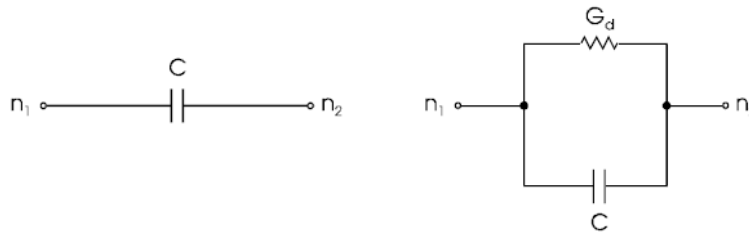
keyword	description	unit	default
<b>R</b>	Resistance	ohm	
<b>TEMP</b>	Local temperature used for noise calculations	K	298
<b>TC1</b>	Temperature coefficient	/degree	0.0
<b>TC2</b>	Temperature coefficient	/degree2	0.0
<b>M</b>	Multiplication factor	1.0	
<b>DTEMP</b>	Temperature difference	degree	0.0

### Notes

1. The default value for **TEMP** is obtained from the value assigned to the global ambient temperature parameter *Tambient* (default, 298 K).

2. If **TC1**, **TC2**, **M** or **DTEMP** is defined, the resistance  $R$  represented by the RES element is given by  $R = R * (1.0 + TC1 * DTEMP + TC2 * DTEMP^2) / M$

## CAP – Capacitor



keyword	description	unit	default
<b>C</b>	Capacitance	farad	
<b>Q</b>	Quality factor, constant conductance model		-
<b>Q1</b>	Quality factor, conductance is proportional to $(1/F)^{EXP}$ . By default, the conductance is proportional to the square root of frequency.		-
<b>Q2</b>	Quality factor, constant- $Q$ model (conductance proportional to frequency)		-
<b>F</b>	Frequency at which the quality factor ( <b>Q</b> , <b>Q1</b> or <b>Q2</b> ) has the assigned value	Hz	
<b>EXP</b>	Quality factor dependence exponent for <b>Q1</b> . The default is $\square 0.5$ ; i.e., the conductance is proportional to the square root of frequency.		0.5
<b>TEMP</b>	Local temperature used for noise calculations	K	298
<b>TC1</b>	Temperature coefficient /degree		0.0
<b>TC2</b>	Temperature coefficient /degree2		0.0
<b>M</b>	Multiplication factor		1.0
<b>DTEMP</b>	Temperature difference	degree	0.0

### Notes

1. The model is described by the following:  $Q(f) = wC / Gd$  where  $w = 2\pi f$  and  $f$  is the operating frequency

2.  $Q(f)$  can be defined as **Q**, **Q1**, or **Q2** respectively. If neither **Q**, **Q1** nor **Q2** is specified, then the capacitor is assumed ideal; that is,  $Gd = 0$ .

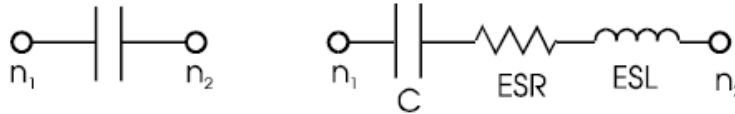
3. Let **QREF**, **Q1REF** and **Q2REF** represent the numeric values of **Q**, **Q1** and **Q2**; that is, the actual number that replaces the symbol. Let **FREF** represent the numeric value of **F**. The frequency dependence of the three *Q* models is given by  $Q: Q(f) = QREF * f/FREF$

$$\begin{aligned} \mathbf{Q1}: Q(f) &= \mathbf{Q1REF} * (\mathbf{FREF}/f)^{\mathbf{EXP}} \\ \mathbf{Q2}: Q(f) &= \mathbf{Q2REF} \end{aligned}$$

4. **EXP** is used in conjunction with **Q1** to define frequency dependence. This parameter defaults to a value of - 0.5, yielding a conductance value that is proportional to the square root of the frequency. The value of **EXP** must be in the range:  $- 6.0 < \mathbf{EXP} < +6.0$

5. If **TC1**, **TC2**, **M**, or **DTEMP** is defined, the capacitance *C* represented by the CAP element is given by  $C = C * (1.0 + \mathbf{TC1} * \mathbf{DTEMP} + \mathbf{TC2} * \mathbf{DTEMP2}) * \mathbf{M}$

### CAPR – Chip Capacitor 3

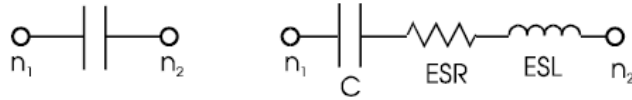


keyword	description	unit	default
<b>C</b>	Capacitance	Farad	0.0
<b>FRES</b>	Self-resonant frequency	Hz	0.0
<b>ESR</b>	Effective Series Resistor	Ohm	0.0
<b>FESR</b>	Frequency at which ESR has assigned a value	Hz	0.0
<b>TC</b>	Temperature Coefficient	PPM	0.0
<b>TEMP</b>	Element temperature	K	298
<b>MOD</b>	Keyword to indicate the name of chip capacitor in a related device library		

#### Notes

1. ESR is Effective Series Resistance.
2. ESL is Effective Series Inductance and can be calculated from the Self-Resonant Frequency FRES
3. TC is defined as PPM (Parts per million). For example, a capacitor has nominal value  $C_0$ , at 298K, at temperature TEMP, the value of the capacitor is calculated as  $C = C_0 * (1 + (TEMP - 298) * TC * 1.0e-6)$

## CAPQ – Chip Capacitor 2



Keyword	description	unit	default
<b>C</b>	Capacitance	Farad	0.0
<b>FRES</b>	Self-resonant frequency	Hz	0.0
<b>Q</b>	Quality Factor		0.0
<b>FQ</b>	Frequency at which ESR has assigned a value	Hz	0.0
<b>TC</b>	Temperature Coefficient	PPM	0.0
<b>TEMP</b>	Element temperature	K	298
<b>MOD</b>	Keyword to indicate the name of chip capacitor in a related device library		

### Notes

1. ESR is Effective Series Resistance and can be calculated from

$$Q \left( ESR = \frac{1}{\omega C * Q} \right)$$

2. ESL is Effective Series Inductance and can be calculated from the Self-Resonant Frequency, FRES

3. TC is defined as PPM (Parts per million). For example, a capacitor has nominal value Co, at 298K, at temperature TEMP, the value of the c

To demonstrate the need of complex elements, here is a practical example of a 6 to 18GHz amplifier simulated with lumped elements.

## 6 to 18 GHz Amp with lumped elements

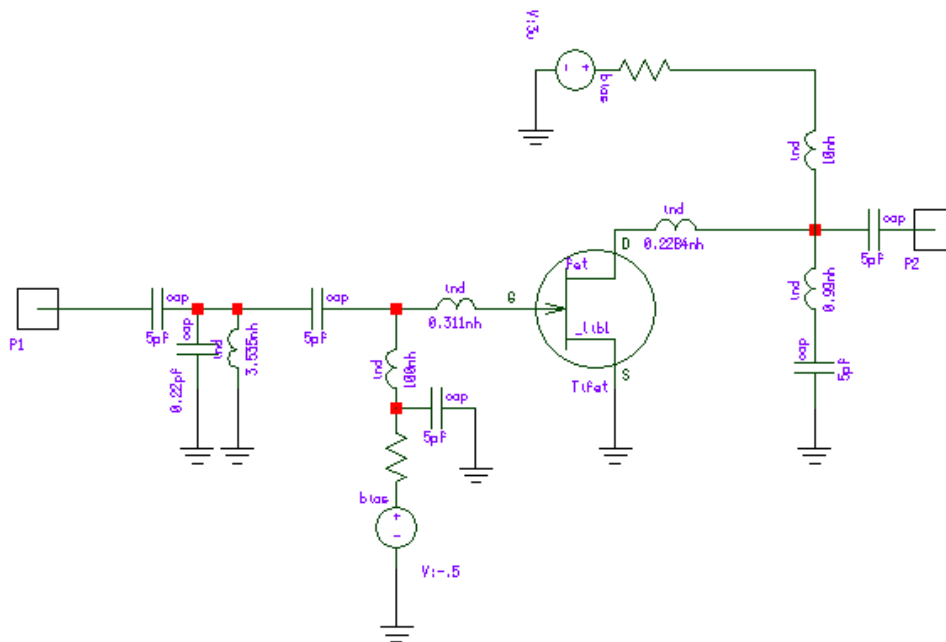


Figure 1 (a): Schematic of 6 to 18GHz Amplifier using Lumped elements

The chosen values were optimized to give a perfect response. To do this of course is silly as the components, based on their parasitic, in reality most definitely have different values.

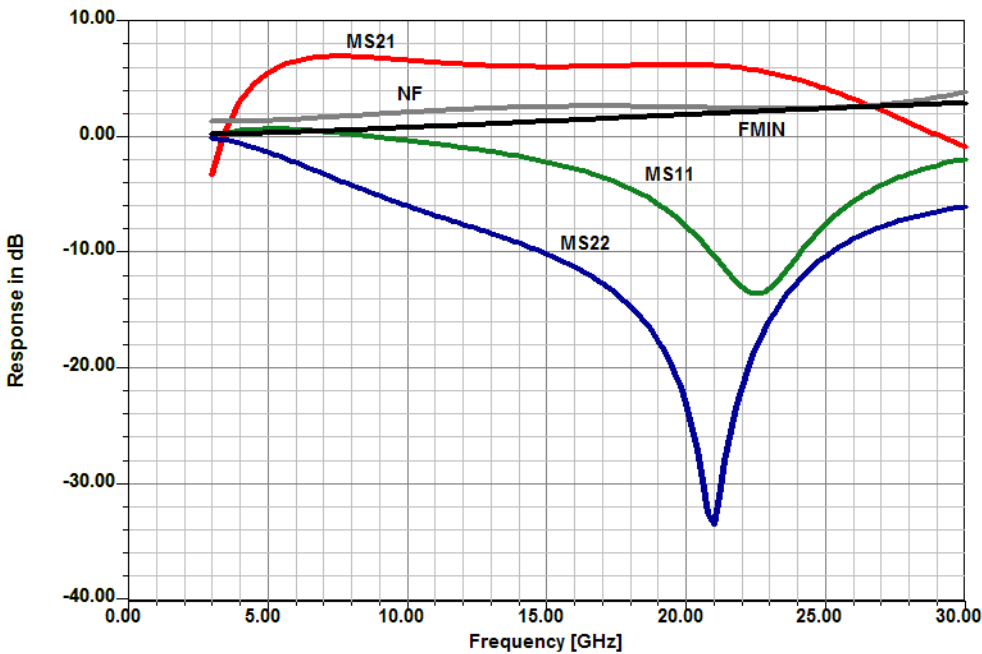


Figure 1 (b): Simulated plot showing the input matching (S11), output matching (S22), Gain (S21) and the  $F_{MIN}$  and NF in dB over the frequency range.

Fig 1 (a) shows the circuit using discrete components to simulate a single stage amplifier. The simulator needs to be able to handle a GaAs model such as the Materka model. And where do the real time domain values come from? However this is not an accurate modeling since the microwave components and junctions elements are missing. The results are too perfect. The minimum noise figure  $F_{min}$  and the actual spot noise figure NF are very low and very close at 25GHz

Now we do the correct simulation and the things change drastically.

# 6 to 18 GHz Amp with Distributed Elements

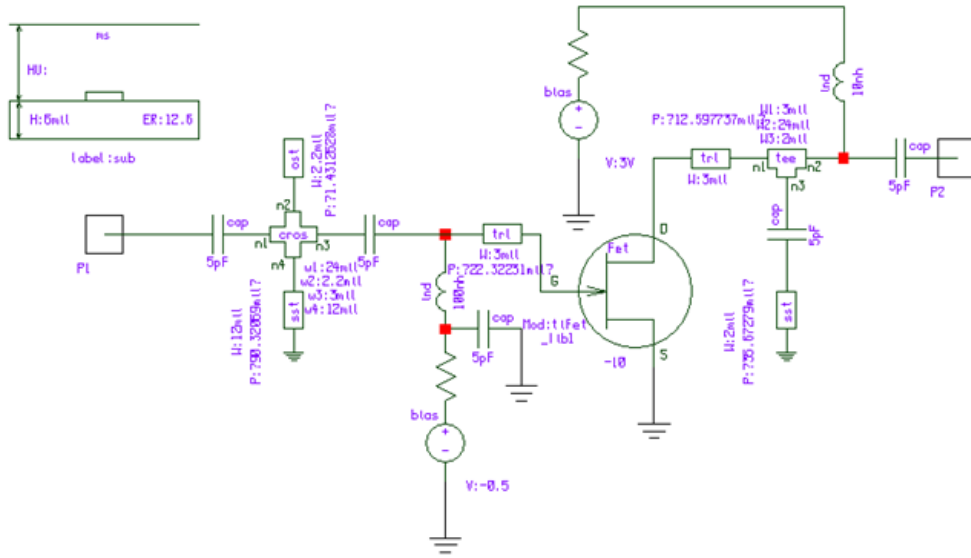


Figure 2 (a): Schematic of 6 to 18GHz Amplifier using Lumped elements

## 1.2 Frequency range above which RF simulators should be used

Figure 2 shows essentially the same circuit but with accurate modeling, and follows the layout reality. This type of circuit goes far beyond any simple SPICE program.

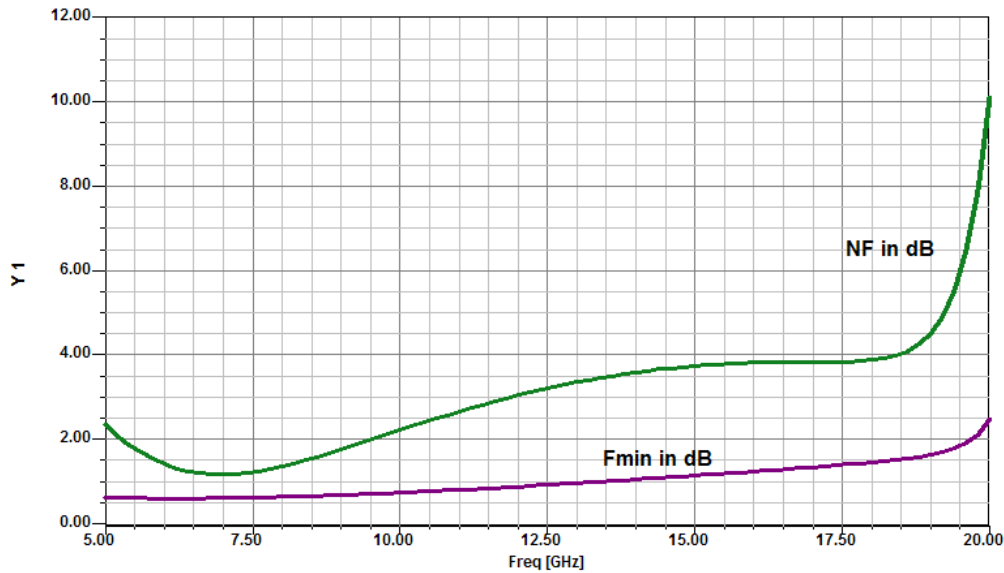


Figure 2 (b): Simulated plot showing the  $F_{\text{MIN}}$  and NF in dB over the frequency range for figure 2(a).

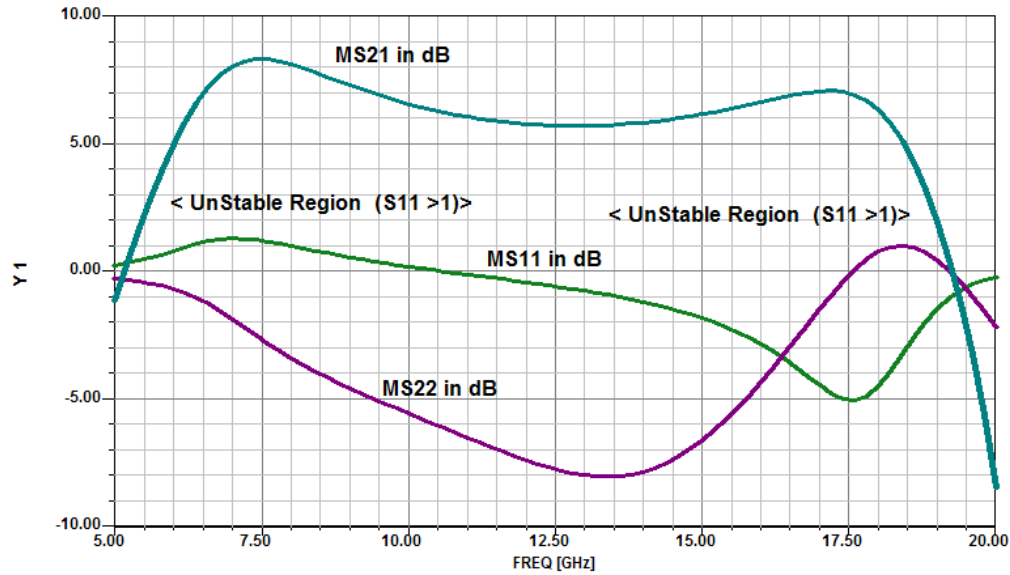


Figure 2 (c): Simulated plot showing the input matching (S11), output matching (S22) and Gain(S21) in dB over the frequency range for Figure 2(a).

### 1.3 Symptoms of low-frequency simulator breakdown

Non-linear programs are also used to predict the nonlinear performance of analog circuits. The following is the mathematical introduction:

**Amplitude Linearity Issues and Figures of Merit.** A network's amplitude nonlinearity can be characterized by the expansion:

$$y = k_1 f(x) + k_2 [f(x)]^2 + k_3 [f(x)]^3 + \text{higher - order terms} \quad (1)$$

where  $y$  represents the output, the coefficients  $k_n$  represent complex quantities whose values can be determined by an analysis of the output waveforms, and  $f(x)$  represents the input. Even though all practical networks exhibit amplitude nonlinearity, we can (and often do) refer to many networks as "linear." We say this of networks that are *sufficiently amplitude-linear for our purposes*--for example, weakly nonlinear networks in which small-signal operation is assumed even though the signal levels involved are sufficient to cause slight distortion. For many practical purposes, the first three terms of (1) adequately describe such a network's nonlinearity:

$$y = k_1 f(x) + k_2 [f(x)]^2 + k_3 [f(x)]^3 \quad (2)$$

In adopting this simplification, we assume also that the nonlinearity is frequency-independent--that is, that the network has sufficient bandwidth to allow all of the products predicted by (1) to appear at its output terminals unperturbed [7].

When multiple signals are present in a network, even weak nonlinearity can result in profound consequences. To illustrate this, we'll let  $f(x)$  consist of two sinusoidal signals:

$$f(x) = A_1 \cos \omega_1 t + A_2 \cos \omega_2 t \quad (3)$$

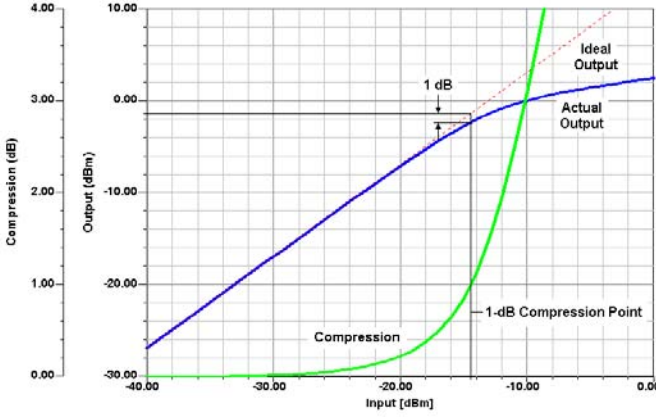


Figure 3: The power level at which a network's power output is down 1 dB relative to that of its ideally linear equivalent is a figure of merit known as the 1-dB compression point (P-1dB). The 1-dB compression point can be expressed relative to input power (P-1dB,in) or output power (P-1dB,out). For the amplifier simulated here, P-1dB,in  $\approx$  -14.5 dBm and P-1dB,out  $\approx$  -1.3 dBm.

We'll assume that  $\omega_1$  and  $\omega_2$  are close enough so that the coefficients  $k_i$  can be considered equal for both signals. We'll also assume for simplicity that all of the  $k_i$  are real. If equation (2) describes the network's response to an input  $f(x)$ , the response will be

$$\begin{aligned}
 y &= k_1(A_1 \cos \omega_1 t + A_2 \cos \omega_2 t) + k_2(A_1 \cos \omega_1 t + A_2 \cos \omega_2 t)^2 + k_3(A_1 \cos \omega_1 t + A_2 \cos \omega_2 t)^3 \\
 &= k_1(A_1 \cos \omega_1 t + A_2 \cos \omega_2 t) \\
 &+ k_2 \left[ A_1^2 \frac{1 + \cos 2\omega_1 t}{2} + A_2^2 \frac{1 + \cos 2\omega_2 t}{2} + A_1 A_2 \frac{\cos(\omega_1 + \omega_2)t + \cos(\omega_1 - \omega_2)t}{2} \right] \\
 &\left\{ \left[ A_1^3 \left( \frac{\cos \omega_1 t}{2} + \frac{\cos \omega_1 t}{4} + \frac{\cos 3\omega_1 t}{4} \right) + A_2^3 \left( \frac{3 \cos \omega_2 t}{4} + \frac{\cos 3\omega_2 t}{4} \right) \right] \right. \\
 &+ k_3 \left. \left\{ \begin{aligned} &+ A_1^2 A_2 \left[ \frac{3}{2} \cos \omega_2 t + \frac{3}{4} \cos(2\omega_1 - \omega_2)t + \frac{3}{4} \cos(2\omega_1 + \omega_2)t \right] \\ &+ A_2^2 A_1 \left[ \frac{3}{2} \cos \omega_1 t + \frac{3}{4} \cos(2\omega_2 + \omega_1)t + \frac{3}{4} \cos(2\omega_2 - \omega_1)t \right] \end{aligned} \right\} \right\} \quad (4)
 \end{aligned}$$

The  $k_1$  term of equation (4) represents the results of amplitude-linear behavior. No new frequency components have appeared; the two sine waves have merely been "rescaled" by  $k_1$ .

The second- and third-order terms of equation (4) represent the effects of harmonic distortion and intermodulation distortion. Second-order effects include second-harmonic distortion (the production of new signals at  $2\omega_1$  and  $2\omega_2$ ) and IMD (the production of new signals at  $\omega_1 + \omega_2$  and  $\omega_1 - \omega_2$ ). Third-order effects include gain compression, third-harmonic distortion (the production of new signals at  $3\omega_1$  and  $3\omega_2$ ), and IMD (the production of new signals at  $2\omega_1 \pm \omega_2$  and  $2\omega_2 \pm \omega_1$ ).

**Gain Compression.** Gain compression occurs when a network cannot increase its output amplitude in linear proportion to an amplitude increase at its input; gain *saturation* occurs when a network's output amplitude stops increasing (in practice, it may actually decrease) with increases in input amplitude. We can deduce from equation (4) that the amplitude of the  $\cos \omega_1 t$  signal has become

$$A'_1 = k_1 A_1 + k_3 \left( \frac{3}{4} A_1^3 + \frac{3}{2} A_1 A_2^2 \right) \quad (5)$$

Because  $k_3$  will normally be negative, a large signal  $A_2 \cos \omega_2 t$  can effectively mask a smaller signal  $A_1 \cos \omega_1 t$  by reducing the network's gain. This third-order effect, known as *blocking* or *desensitization* when it occurs in a receiver, is a special case of gain compression. The presence of additional signals results a greater reduction in gain; the gain reduction for each signal is a function of the relative levels of all signals present. A receiver's blocking behavior may be characterized in terms of the level of off-channel signal necessary to reduce the strength of an in-passband signal by a specified value, typically 1 dB; alternatively, the decibel ratio of the off-channel signal's power to the receiver's noise-floor power may be cited as *blocking dynamic range*. Desensitization may be also characterized in terms of the off-channel-signal power necessary to degrade a system's SNR by a specified value.

Multiple signals need not be present for gain compression to occur. If only one signal is present, the ratio of gain with distortion to the network's idealized (linear) gain is

$$A'_1 = \frac{k_1 + k_3 \left( \frac{3}{4} A_1^2 \right)}{k_1} \quad (6)$$

This is referred to as the *single-tone gain-compression factor*. Figure 3 shows how the  $k_3$  term causes a network's gain to deviate from the ideal. The point at which a network's power gain is down 1 dB from the ideal for a single signal is a figure of merit known as the *1-dB compression point* ( $P_{-1dB}$ ). Many networks (including many receiving and low-level transmitting circuits, such as low-noise amplifiers, mixers and IF amplifiers) are usually operated under small-signal conditions--at levels sufficiently below  $P_{-1dB}$  to maintain high linearity. As we'll see, however, some networks (including power amplifiers for wireless systems) may be operated under large-signal conditions – near or in compression – to achieve optimum efficiency at some specified level of linearity.

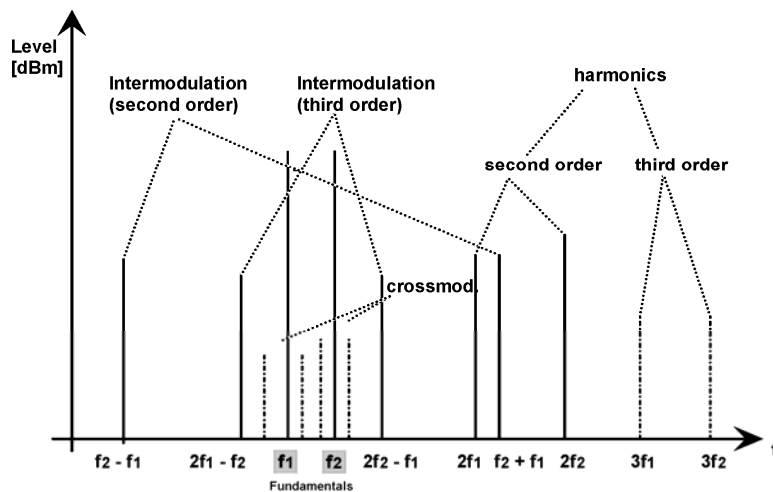


Figure 4: Relationships between fundamental and spurious signals, including harmonics and products of intermodulation.

**Intermodulation.** The new signals produced through intermodulation distortion (IMD) can profoundly affect the performance even of systems operated far below gain compression (Figure 4). IMD products of significant power can appear at frequencies remote from, in and/or near the system passband, resulting in demodulation errors (in reception) and interference to other communications (in transmission). Where an IMD product appears relative to the passband depends on the passband width and center frequency, the frequencies of the signals present at the system input, and the order of the nonlinearity involved. These factors also determine the strength of an IMD product relative to the desired signal.

Second-order IMD (IM<sub>2</sub>) results, for an input consisting of two signals  $\omega_1$  and  $\omega_2$ , in the production of new signals at  $\omega_1 + \omega_2$  and  $\omega_1 - \omega_2$ ; third-order IMD (IM<sub>3</sub>) results, for an input consisting of two signals  $\omega_1$  and  $\omega_2$ , in the production of new signals at  $2\omega_1 \pm \omega_2$  and  $2\omega_2 \pm \omega_1$ .

Under small-signal conditions--that is, at levels well below compression--the power of an IM<sub>2</sub> product varies by 2 dB, and the power of an IM<sub>3</sub> product varies by 3 dB, per decibel change in input power level. This allows us to derive a network figure of merit, the *intermodulation intercept point (IP)*, for a given IM order by extrapolating a network's linear and IM responses to their point of intersection (Figure 5) – the point at which their powers would be equal if compression did not occur. Because of the system noise and/or intermodulation distortion products, there is a minimum discernible signal (MDS) that limits the dynamic range at the lower end. Theoretically, Figure 5 should show a noise floor or IMD-spur floor for a given input signal that represents a lower limit below which signals cannot be detected. The intercept point for a given IM order  $n$  can be expressed, and should always be characterized, relative to input power (IP<sub>*n*,in</sub>) or output power (IP<sub>*n*,out</sub>); the IP<sub>in</sub> and IP<sub>out</sub> values differ by the network's linear gain. For equal-level test tones, IP<sub>*n*,in</sub> can be determined by:

$$IP_{n,in} = \frac{nP_A - P_{IM_n}}{n-1} \quad (7)$$

where  $n$  is the order,  $P_A$  is the input power (of one tone),  $P_{IM_n}$  is the power of the IM product, and  $IP$  is the intercept point. The intercept point for cascaded networks can be determined from

$$IP_{2,in} = \frac{1}{\left(\frac{1}{\sqrt{IP_1}} + \frac{G}{\sqrt{IP_2}}\right)^2} \quad (8)$$

for IP<sub>2</sub> and from

$$IP_{3,in} = \frac{1}{\frac{1}{IP_1} + \frac{G}{IP_2}} \quad (9)$$

for IP<sub>3</sub>. In both equations,  $IP_1$  is the input intercept of Stage 1 in watts,  $IP_2$  is the input intercept of Stage 2 in watts, and  $G$  is the gain of Stage 1 (as a numerical ratio, *not* in decibels). Both equations assume the worst-case condition, in which the distortion products of both stages add in-phase.

The ratio of the signal power to the IM-product power, the *distortion ratio*, can be expressed as:

$$R_{dn} = (n-1) \left[ IP_{n(in)} - P_{(in)} \right] \quad (10)$$

where  $n$  is the order,  $R_{dn}$  is the distortion ratio,  $IP_{n(in)}$  is the input intercept point, and  $P_{(in)}$  is the input power of one tone.

Discussions of IMD have traditionally downplayed the importance of  $IM_2$  because the incidental distributed filtering contributed by the tuned circuitry once common in radio communication systems was usually enough to render out-of-passband  $IM_2$  products caused by in-passband signals, and in-passband  $IM_2$  products caused by out-of-passband signals, vanishingly weak compared to fundamental and  $IM_3$  signals. In broadband systems that operate at bandwidths of an octave or more, however, in-passband signals may produce significantly strong in-passband  $IM_2$  and second-harmonic products. In such applications, balanced circuit structures (such as push-pull amplifiers and balanced mixers) can be used to minimize  $IM_2$  and other even-order nonlinear products.

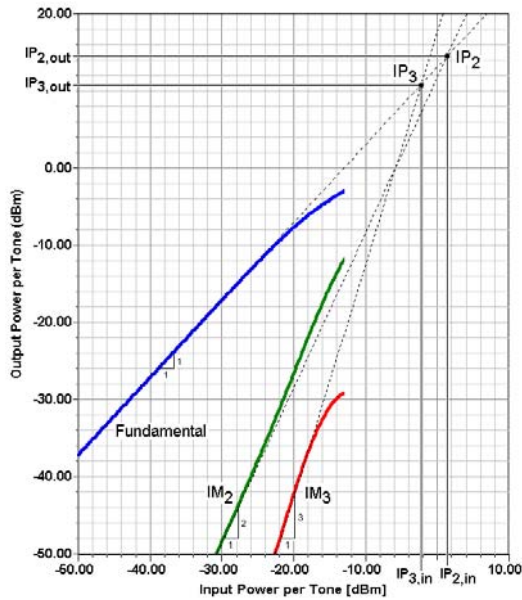


Figure 5: The level at which the power of one of a network's IM products equals that of the network's linear output is a figure of merit known as the intermodulation intercept point (IP). The intercept point for a given IM order  $n$  can be expressed, and should always be characterized, relative to input power ( $IP_n, in$ ) or output power ( $IP_n, out$ ); the  $IP_{in}$  and  $IP_{out}$  values differ by the network's linear gain. For the amplifier simulated here,  $IP_{2,in} \approx 1.5$  dBm,  $IP_{2,out} \approx 14.5$  dBm,  $IP_{3,in} \approx -2.3$  dBm and  $IP_{3,out} \approx 10.7$  dBm. Each curve depicts the power in one tone of the response evaluated.

As with  $IM_2$ , which  $IM_3$  products are important depends on the spacing of the signals involved and the relative width of the system passband. If  $\omega_1$  and  $\omega_2$  are of approximately the same frequency, the additive products  $2\omega_1 + \omega_2$  and  $2\omega_2 + \omega_1$  will be outside the passband of a narrowband system. The subtractive products  $2\omega_1 - \omega_2$  and  $2\omega_2 - \omega_1$ , however, will likely appear near or within the system passband. The  $IM_3$  performance of any network subjected to multiple signals is therefore of critical importance, and an array of  $IM_3$ -related, sometimes application-specific, figures of merit has evolved as a result.

**Dynamic Range.** As we have seen, thermal noise sets the lower limit of the power span over which a network can operate. Distortion--that is, degradation by distortion of the signal's ability to convey information--sets the upper limit of a network's power span. Because the power level at which distortion becomes intolerable varies with signal type and application, a generic definition has evolved: The upper limit of a network's power span is the level at which the power of one IM product of a specified order is equal in power to the network's noise floor. The ratio of the noise-floor power to the upper-limit signal power is referred to as the network's *dynamic range (DR)*, often more

carefully characterized as *two-tone IMD dynamic range*, which, when evaluated with equal-power test tones, is a figure of merit commonly used to characterize receivers. The MDS relative to the input, as already defined, is

$$\text{MDS}_{\text{in}} = kTB + 3 \text{ dB} + \text{NF}$$

When  $\text{IP}_{(n)\text{in}}$  and MDS are known, IMD DR can be determined from:

$$\text{DR}_n = \frac{(n-1)[\text{IP}_{n(\text{in})} - \text{MDS}_{\text{in}}]}{n} \quad (11)$$

where  $DR$  is the dynamic range in decibels,  $n$  is the order,  $\text{IP}_{(in)}$  is the input intercept power in dBm, and MDS is the minimum detectable signal power in dBm. The so-called *spurious-free dynamic range* ( $\text{SFDR}$  or  $\text{DR}_{\text{SF}}$ ) is calculated from

$$\text{DR}_{\text{SF}} = \frac{2}{3}(\text{IP}_3 - 174 \text{ dBm} + \text{NF} + 3 \text{ dB})$$

This equation allows us to determine how to measure the spurious-free dynamic range. This is done by applying the two-tone signals (in the case of  $\text{IP}_3$ ) and increasing the two signals to the point where the signal-to-noise ratio deteriorates by 3 dB or, if the measurement is done relative to MDS, where the noise floor rises by 3 dB. The factor 2/3 is derived from the fact that the levels of  $\text{IM}_3$  outputs increase 3 dB for 1 dB of input increase. This definition of dynamic range now is referenced to a noise figure rather than a minimum level in dBm, and is therefore independent of bandwidth. (By choosing smaller bandwidths [1 kHz instead of 10 kHz], a dynamic range measurement can be made to look better. Basing the specification on noise figure directly avoids this problem.)

#### 1.4 An important test example:

Modern signals are multitone signals and according to international standards sensitive circuits such as CATV amplifiers must be specified in this area. Figure 6 shows the circuit diagram of such a circuit in this case a distribute amplifier.

Its frequency range is from 3GHz to 21GHz. The figure 6 shows how the simulation is organized and since all modern SPICE programs use schematic entries other simulators may do it different but essentially the same way.

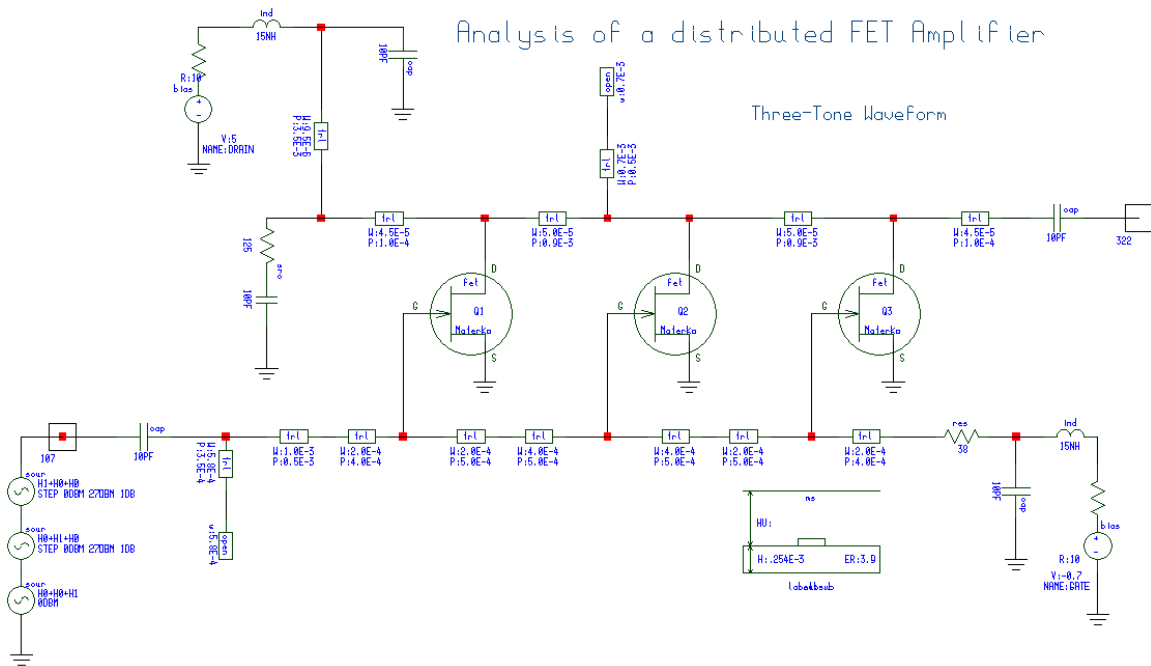


Figure 6: Circuit diagram of the distributed amplifier for 3 to 21GHz

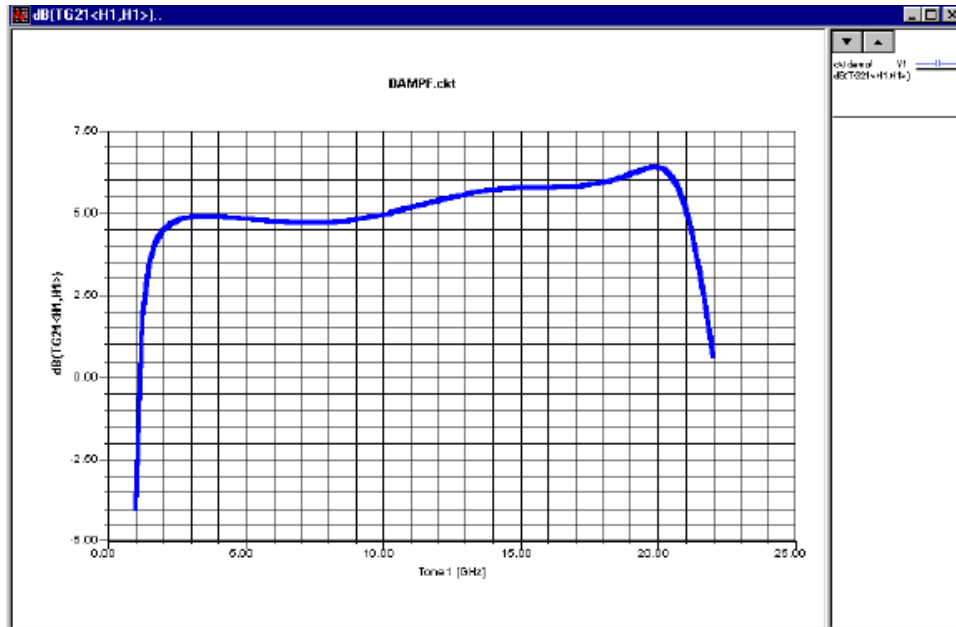


Figure 7: Output gain of the amplifier as predicted over the operating sweep range.

Figure 7 shows the resulting predicted gain plot for the amplifier in the Figure 6. Non-linear circuits respond differently and figure 8 shows some predicted and measured data. [10]

### ***Triple-Beat Distortion and Cross-Modulation.***

$P_{-1dB}$  is a single-tone figure of merit; blocking, intercept point and dynamic range evaluate two-tone behavior. For networks that must handle AM and composite (AM and angle modulation) signals very linearly, such as television transmitters and cable TV distribution systems, a three-tone figure of merit called *triple-beat distortion*

has gained acceptance. Signals at  $\omega_1$  and  $\omega_2$  (closely spaced) and  $\omega_3$  (positioned far away from  $\omega_1$  and  $\omega_2$ ) are applied to the network under test, at levels, frequencies and spacings that vary with the application. One triple-beat distortion figure of merit is the ratio, expressed in decibels, of the IM product at  $\omega_3 + (\omega_2 - \omega_1)$  to one of the network's linear outputs at a specified output level. Alternatively, the triple-beat figure of merit may express the network output level at which a specified triple-beat ratio occurs.

Triple-beat distortion is the mechanism underlying cross-modulation, a form of intermodulation in which one or more AM signals present in a network amplitude-modulate all signals present in the network [8]. Figures 8a and 8b graph the results of gain compression, two-tone intermodulation, cross-modulation and triple-beat testing on a wideband (5 to 1000 MHz) amplifier.

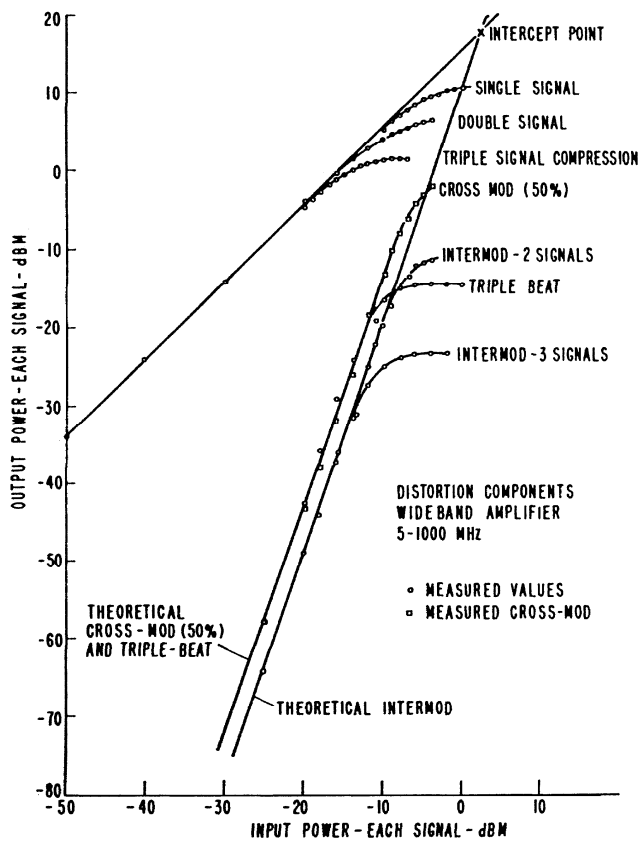


Figure 8a: Measured distortion components in a wideband (5 to 1000 MHz) amplifier. Figure 8b shows a magnified view of the gain-compression region [9].

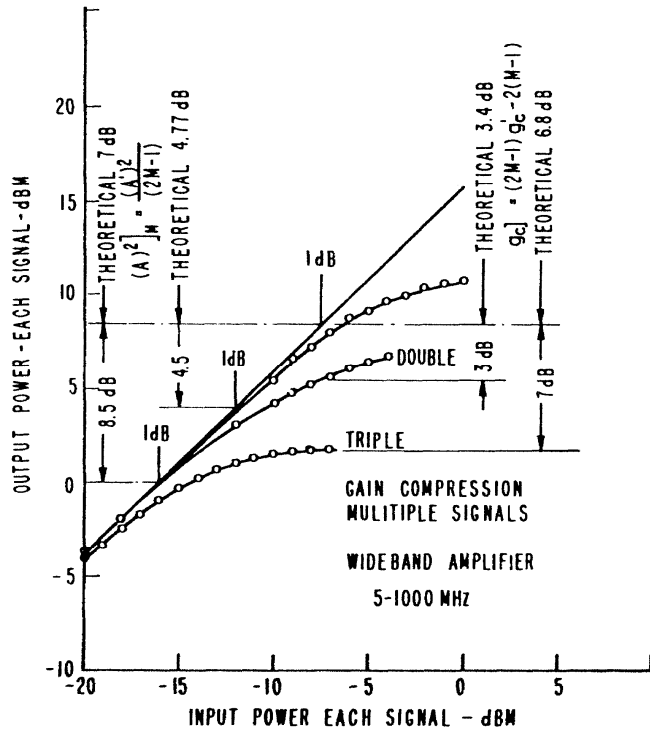


Figure 8b: Measured multiple-signal gain compression of the 5- to 1000-MHz amplifier [9].

How to determine that a conventional simulator tool is unsuitable? One type of breakdown is the question of convergence, the simulator will give an error advising the numerical problem, but mostly not giving a solution. The next problem is the missing components as shown above. Or the question about noise figure of amplifiers or phase noise of an oscillator cannot be answered by a SPICE program accurately.

To satisfy for our queries we have taken the following examples. The first one is a 4GHz amplifier designed using CMOS technology. One transistor is used for biasing and the other two forms a cascade for stability shown in Figure 9(a). The inductor in the source of the FET3 makes close matching of a low noise figure and a good S11 (power) matching possible. This is an application case for simulator testing, but cannot build like this practically.



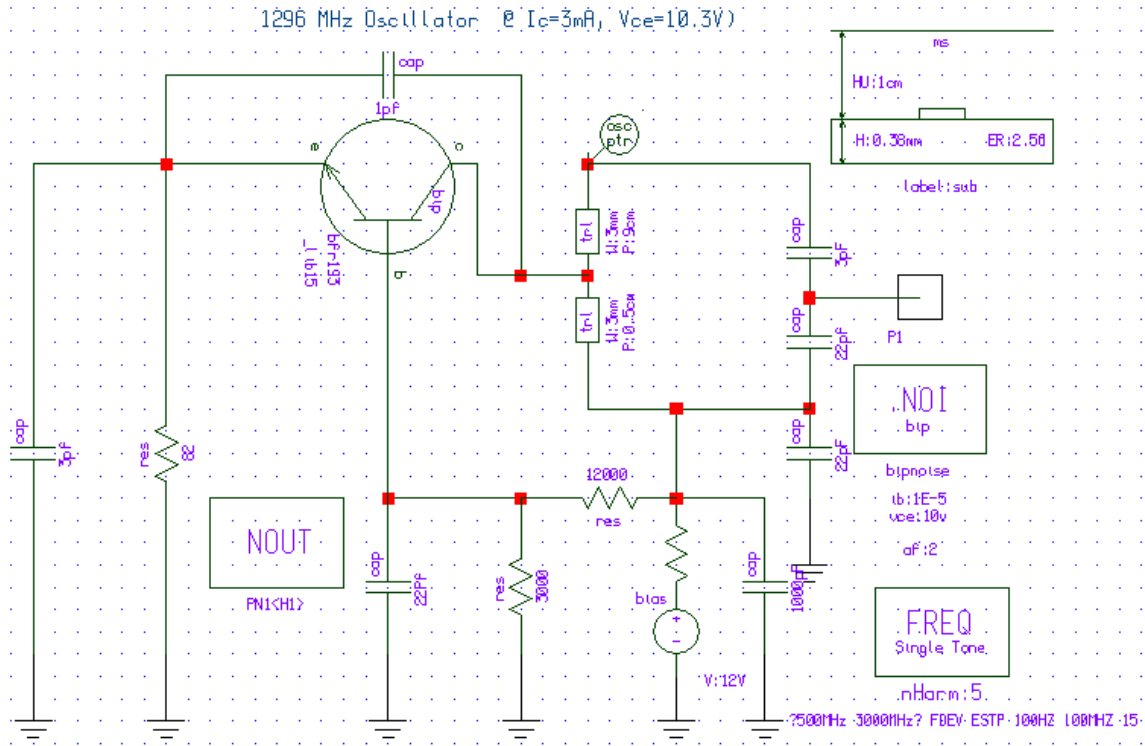


Figure 10 (a): Schematic of 1296MHz oscillator

The oscillator is a standard grounded base arrangement using transmission lines as resonators. The next two figures plotted in simulation tool show the predicted output power and harmonic content as well as the phase noise.

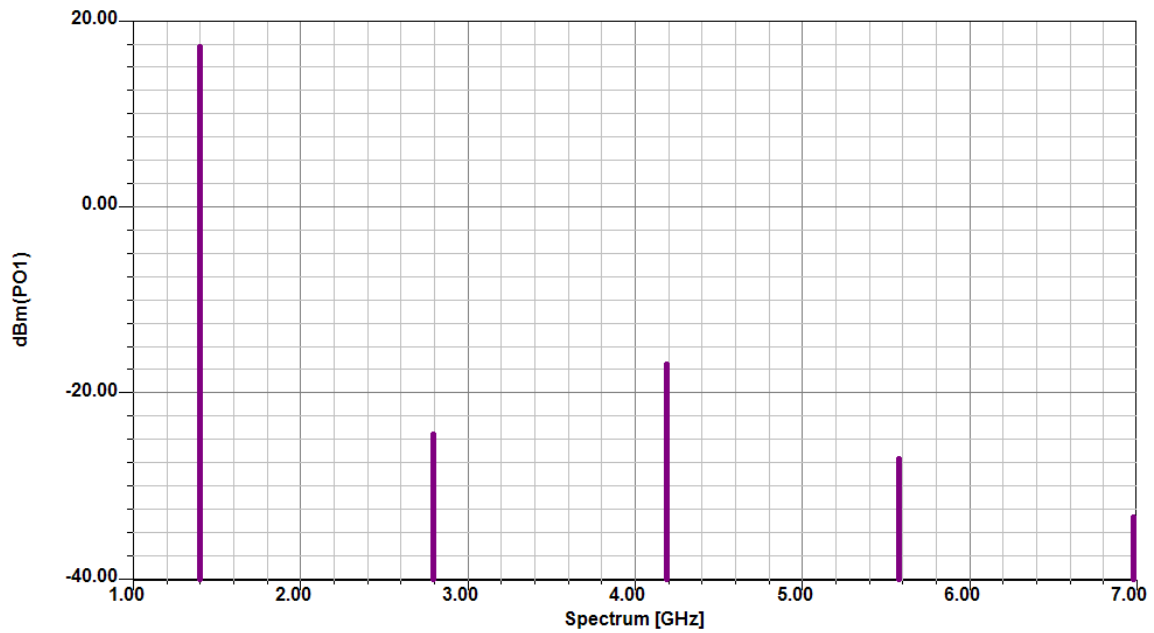


Figure 10 (b): Simulated plot showing the harmonic content and the predicted output power for the 1296 MHz oscillator

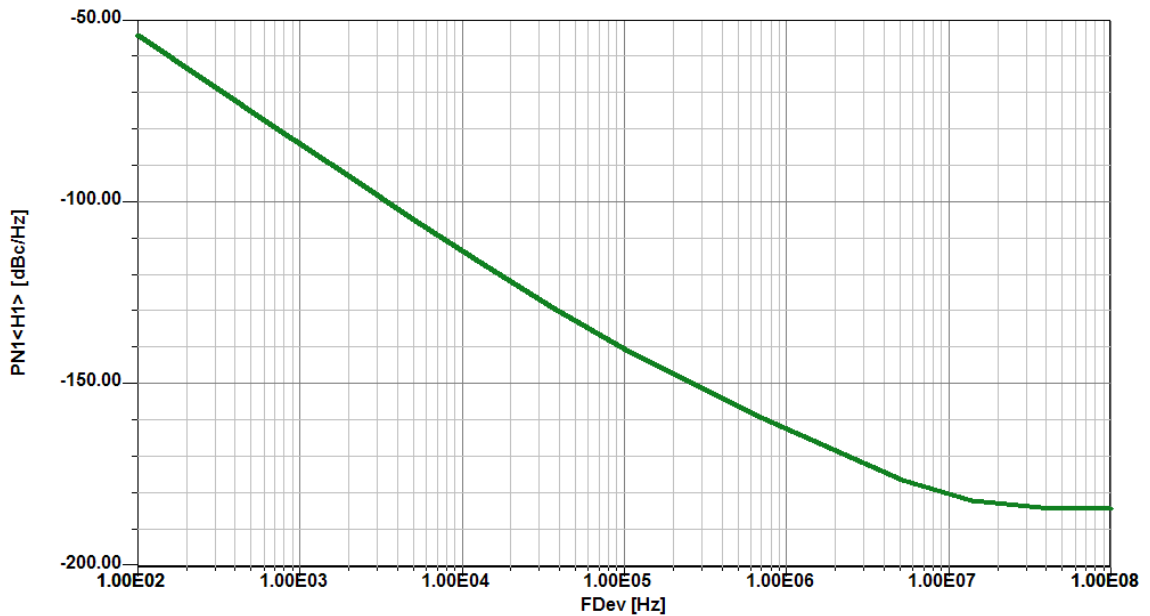


Figure 10 (c): Simulated plot showing the predicted phase noise for schematic in figure 10(a)

The following time domain analysis using the enhanced technique is a good example showing the progress. A microwave oscillator is keyed on and off and a transient analysis is performed. This is shown in the next figure.

When using the standard SPICE based on SPICE3, the initial calculation shows a wrong response after one iteration, see the following figure. It takes about 80 pulses (80<sup>th</sup> period of the pulsed drain voltage) until the simulation follows the Krylov-subspace based HB and gives a correct answer. (See Appendix 1 – Krylov-subspace) The speed improvement is 11 times faster and the required memory is about 10%

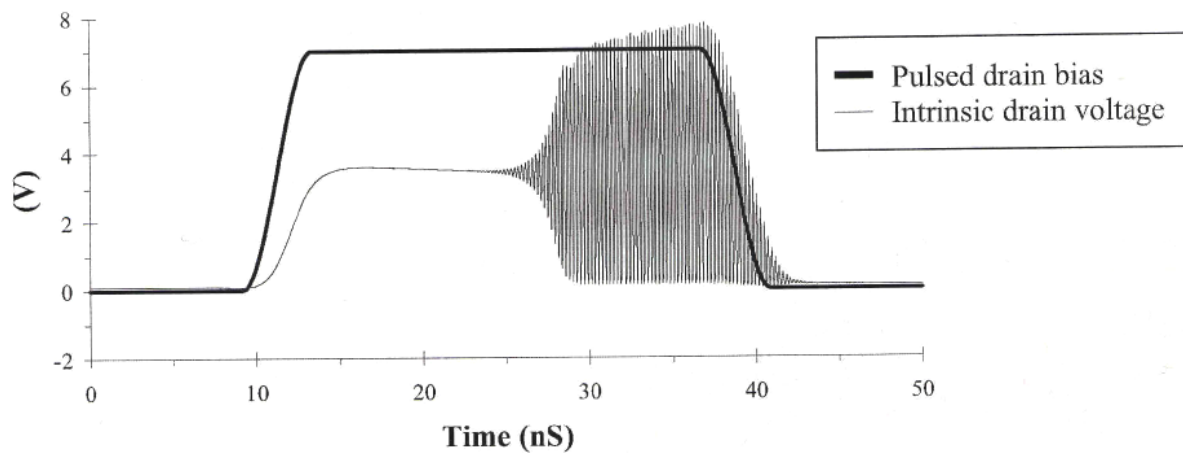


Figure 11 (a): Krylov-subspace based HB result

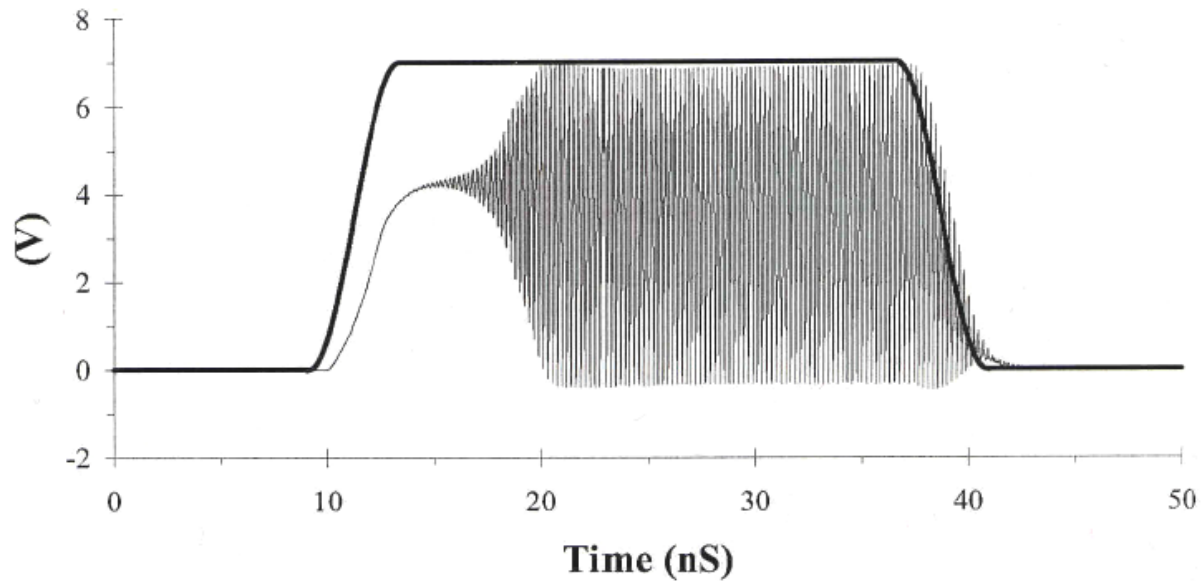


Figure 11 (b): Standard SPICE result

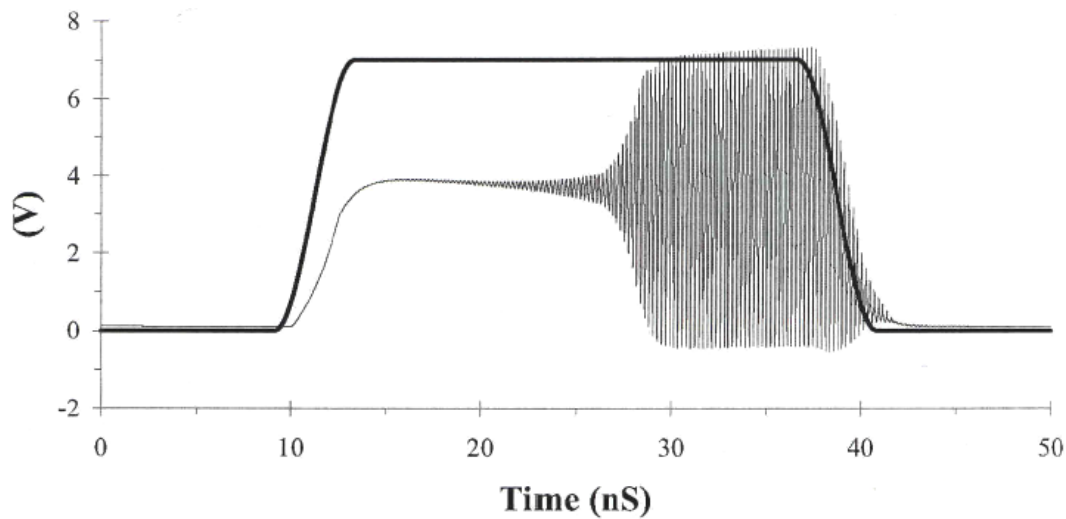


Figure 11 (c): 80 iterations later the result of the standard SPICE provides the same result as the Krylov-subspace solution.

The next picture, Figure 12, shows the transient performance relative to  $V_{be}$  as oscillation occurs. At the time  $t=0$  the base emitter is the standard 600mV. After a short time oscillation tries to start and there is a DC shift, based on the biasing network impedance and capacitance. At the steady state value, there is the RF riding on a reduced DC voltage which is responsible of the amplitude stabilization. This is a nice application for RF analysis. Using quartz crystals, this can be a high as a few seconds based on the Q of 1 million or more.

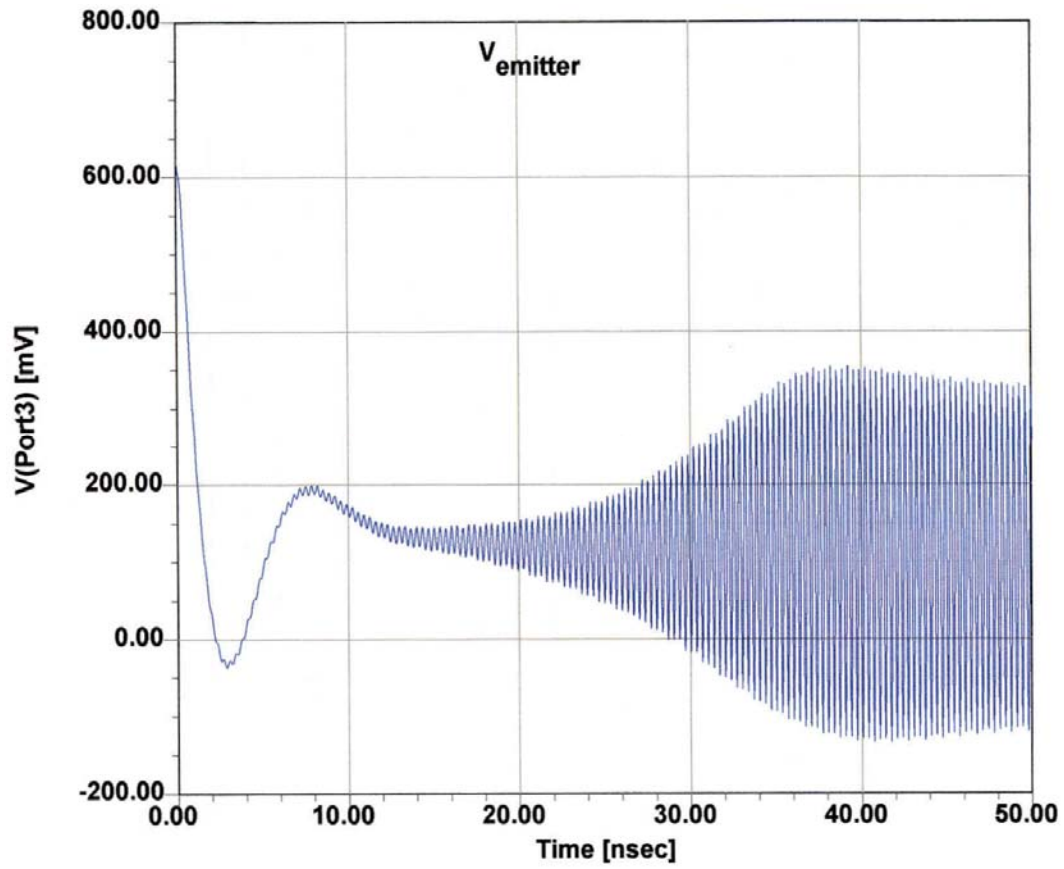


Figure 12: Transient response relative to  $V_{be}$

## 2. RF SIMULATION TOOLS AND TECHNOLOGY

### 2.1 RF simulator technology overview

RF simulators fall in the categories of SPICE, HB programs and EM (electromagnetic) programs. The EM simulators are more exotic programs. Two types are common, the 2 (2.5)D and the full 3D versions. They are used to analyze planar circuits, including Vias (ground connections) or wrap arounds, top to ground plane side connections. The 3D simulator helps with transitions or other crosstalk or resonant conditions. We will not address these here as they go far beyond the SPICE concept.

The modern HB programs have found better solutions for both handling a very large number of transistors, up to 1 million and even more and handle the math solutions now much more efficient. Memory management and solving non-linear equations for transient analysis are some of the key factors. HB analysis performs steady-state analysis of periodically excited circuits. The circuit to be analyzed is split into linear and nonlinear subcircuits. The linear subcircuit is calculated in the frequency domain. Features of this aspect of the HB process include:

- Use of distributed models in the spectral domain
- Matrix formulation that can enable reduction of internal nodes
- Major speed advantage
- Straightforward intermodulation and mixer analysis

The nonlinear subcircuit is calculated in the time domain. Features of this aspect of the HB process include:

- Nonlinear models derived directly from device physics
- Intuitive, easy and logical circuit representation

Figure 13 diagrams this approach for a MESFET amplifier. Figure 14 charts a general-purpose nonlinear design algorithm that includes optimization. Modern analysis tools that must provide accurate phase-noise calculation should be based on the principle of harmonic balance. In Section 8, Application 2, Figure 46 shows a BJT microwave oscillator entered into the schematic-capture module of a commercially available HB simulator (Ansoft Serenade 8.0); Figure 47 shows this oscillator's simulated phase noise. By the way, HB analysis can also handle mixers.

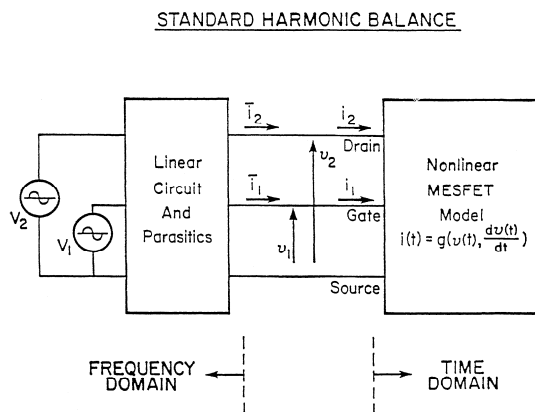


Figure 13: MESFET circuit partitioned into linear and nonlinear subcircuits for harmonic-balance analysis. Applied gate and drain voltages, and relevant terminal voltages and currents, are indicated.

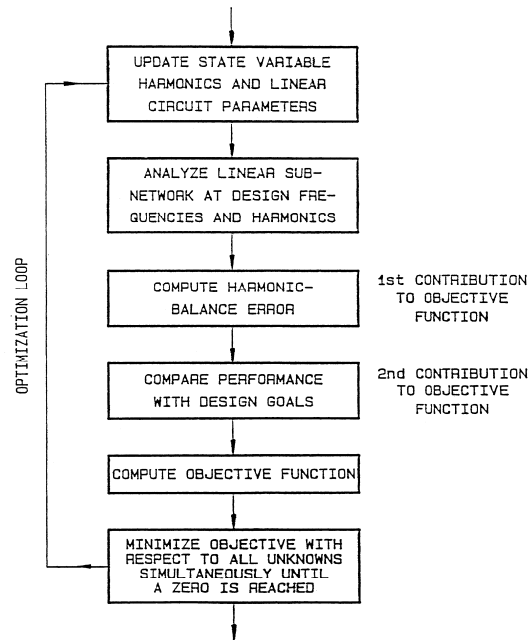


Figure 14: Flowchart of a general-purpose harmonic-balance design algorithm that includes optimization.

Transient analysis in microwave oscillators includes problems of primary importance such as oscillation buildup at bias turn-on and frequency settling in VCOs. Until now this class of problems has been tackled by two families of algorithms, i.e., either rigorous but computationally inefficient time-domain methods, or fast but approximate envelope-oriented techniques. It has been shown that an excellent trade-off retaining the advantages of both the above without significant shortcomings may be achieved by Krylov-subspace based inexact-Newton harmonic-balance (INHB) analysis.

### 3. EXAMPLES OF RF SIMULATION TOOLS, PROFESSIONAL AND STUDENT/HOBBYIST

**PSPICE:** This popular version of SPICE, available from Orcad (now Cadence) runs under the PC and Macintosh platforms. An evaluation version, which can handle small circuits with up to 10 transistors, is freely available. For a full fledged version or for more information, please contact Orcad. AIM-SPICE is a pc-version of SPICE with a revised user interface, simulation control, and with extra models. A student version can be downloaded. A complete list of all SPICE offerings (and software downloads for a wide range of platforms).

This student version, from my experience, is the best on the market. There are a number of PC-based SPICE programs in the \$1000 region but they are more for switching power supplies and logic circuit optimization than RF. Here are two important programs:

[www.intusoft.com/demos.htm](http://www.intusoft.com/demos.htm)

[www.spectrum-soft.com/index.shtm](http://www.spectrum-soft.com/index.shtm)

**HSPICE:**

- RF and High Speed Simulation
- Best RF Simulator for PLL and VCO applications
- Most Accurate RF Simulator
- Fastest RF Simulator
- High Capacity RF Simulator, 10000+ transistors with both Harmonic Balance and Shooting Newton algorithms
- Comprehensive solution simulates low noise amplifiers, power amplifiers, filters, AGC circuits, oscillators, mixers, multipliers, modulators, demodulators, and VCOs.

Agilent, AWR and Ansys offer very modern CAD tools, mixed mode, and they combine the concept of SPICE and the advanced technologies. The question remains of where to obtain RF models?

## 4. SPECIFIC AREAS OF CONCERN

### 4.1 Noise

Here we need to look at the noisy two-port description and the application of the noise correlation matrix, which only the harmonic balanced based or hybrid (SPICE) programs have.

**Noisy Two-Port Description:** Based on the convention by Rothe and Dalke [12], any linear two-port can be in the form shown in Figure 15(a, b, c). This general case of a noisy two-port can be redrawn showing noise sources at the input and at the output. Figure 15(b) shows this in admittance form and Figure 15(c) in impedance form. The internal noise sources are assumed to produce very small currents and voltages, and we assume that linear two-port equations are valid. The internal noise contributions have been expressed by using external noise sources:

$$\begin{aligned} I_1 &= y_{11}V_1 + y_{12}V_2 + I_{K1} \\ I_2 &= y_{21}V_1 + y_{22}V_2 + I_{K2} \end{aligned} \quad (12)$$

$$\begin{aligned} V_1 &= z_{11}I_1 + z_{12}I_2 + V_{L1} \\ V_2 &= z_{21}I_1 + z_{22}I_2 + V_{L2} \end{aligned} \quad (13)$$

where the external noise sources are  $I_{K1}$ ,  $I_{K2}$ ,  $V_{L1}$ , and  $V_{L2}$ .

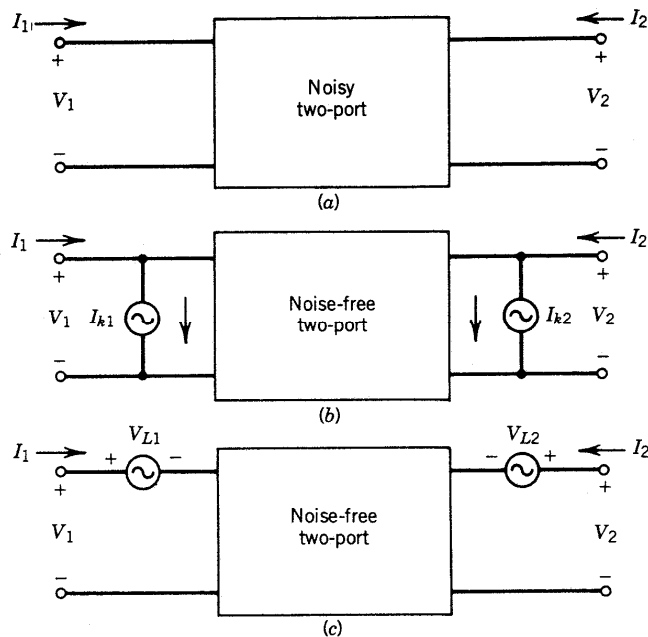


Figure 15: Noise linear two-ports: (a) general form; (b) admittance form; (c) impedance form.

Since we want to describe our noisy circuit in terms of the noise figure, the  $ABCD$ -matrix description will be more convenient since it refers both noise sources to the input of the two-port [13]. This representation is given below (note the change in direction of  $I_2$ ):

$$\begin{aligned}
V_1 &= AV_2 + BI_2 + V_A \\
I_1 &= CV_2 + DI_2 + I_A
\end{aligned}
\tag{14}$$

where  $V_A$  and  $I_A$  are the external noise sources.

It is important to remember that all of these matrix representations are interrelated. For example, the noise noises for the  $ABCD$ -matrix description can be obtained from the  $z$ -matrix representation shown in (13). This transformation is

$$V_A = -\frac{I_{K2}}{y_{21}} = V_{L1} - \frac{V_{L2}z_{11}}{z_{21}}
\tag{15}$$

$$I_A = I_{K1} - \frac{I_{K2}y_{11}}{y_{21}} = -\frac{V_{L2}}{z_{21}}
\tag{16}$$

The  $ABCD$  representation is particularly useful based on the fact that it allows us to define a noise temperature for the two-port referenced to input. The two-port itself (shown in Figure 16) is assumed to be noise-free.

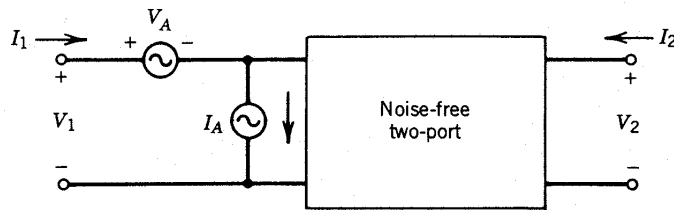


Figure 16: Chain-matrix form of linear noisy two-ports.

In the past,  $z$  and  $y$  parameters have been used, but in microwave applications it has become common to use  $S$ -parameter definitions. This is shown in Figure 17. The previous equations can be rewritten in their new form using  $S$  parameters:

$$\begin{bmatrix} b_1 \\ b_2 \end{bmatrix} = \begin{bmatrix} S_{11} & S_{12} \\ S_{21} & S_{22} \end{bmatrix} \begin{bmatrix} a_1 \\ a_2 \end{bmatrix} + \begin{bmatrix} b_{n1} \\ b_{n2} \end{bmatrix}
\tag{17}$$

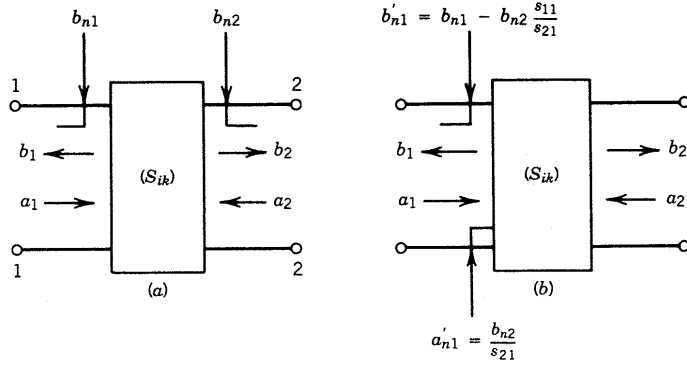


Figure 17: S-parameter form of linear noisy two-ports.

There are different physical origins for the various sources of noise. Typically, thermal noise is generated by resistances and loss in the circuit or transistor, whereas shot noise is generated by current flowing through semiconductor junctions and vacuum tubes. Since these many sources of noise are represented by only two noise sources at the device input, the two equivalent noise sources are often a complicated combination of the circuit internal noise sources. Often, some fraction of  $V_A$  and  $I_A$  is related to the same noise source. This means that  $V_A$  and  $I_A$  are not independent in general. Before we can use  $V_A$  and  $I_A$  to calculate the noise figure of the two-port, we must calculate the correlation between the  $V_A$  and  $I_A$  shown in Figure 16.

The noise source  $V_A$  represents all the device noise referred to the input when the generator impedance is zero; that is, when the input is short-circuited. The noise source  $I_A$  represents all the device noise referred to the input when the generator admittance is zero; that is, the input in open-circuited.

The correlation of these two noise sources considerably complicates analysis. By defining a correlation admittance, we can simplify the mathematics and get some physical intuition for the relationship between noise figure and generator admittance. Since some fraction of  $I_A$  will be correlated with  $V_A$ , we split  $I_A$  into correlated and uncorrelated parts as follows:

$$I_A = I_n + I_u \tag{18}$$

$I_u$  is the part of  $I_A$  uncorrelated with  $V_A$ . Since  $I_n$  is correlated with  $V_A$ , we can say that  $I_n$  is proportional to  $V_A$  and the constant of proportionality is the correlation admittance.

$$I_n = Y_{\text{cor}} V_A \tag{19}$$

This leads us to

$$I_A = Y_{\text{cor}} V_A + I_u \tag{20}$$

The following derivation of noise figure will use the correlation admittance.  $Y_{\text{cor}}$  is not a physical component located somewhere in the circuit.  $Y_{\text{cor}}$  is a complex number derived by correlating the random variables  $I_A$  and  $V_A$ . To calculate  $Y_{\text{cor}}$ , we multiply each side of (20) by  $V_A^*$  and average the result. This gives

$$\overline{V_A^* I_A} = Y_{\text{cor}} \overline{V_A^2} \quad (21)$$

where the  $I_u$  term averaged to zero since it was uncorrelated with  $V_A$ . The correlation admittance is thus given by

$$Y_{\text{cor}} = \frac{\overline{V_A^* I_A}}{\overline{V_A^2}} \quad (22)$$

Often, people use the term "correlation coefficient." This normalized quantity is defined as

$$c = \frac{\overline{V_A^* I_A}}{\sqrt{\overline{V_A^2} \overline{I_A^2}}} = Y_{\text{cor}} \sqrt{\frac{\overline{V_A^2}}{\overline{I_A^2}}} \quad (23)$$

Note that the dual of this admittance description is the impedance description. Thus the impedance representation has the same equations as above with  $Y$  replaced by  $Z$ ,  $I$  replaced by  $V$  and  $V$  replaced by  $I$ .

$V_A$  and  $I_A$  represent internal noise sources in the form of a voltage source acting in series with the input voltage and a source of current flowing in parallel with the input current. This representation conveniently leads to the four noise parameters needed to describe the noise performance of the two-port. Again using the Nyquist formula, the open-circuit voltage of a resistor at the temperature  $T$  is

$$\overline{V_A^2} = 4kTRB \quad (24)$$

This voltage is a mean-square fluctuation (or spectral density). It is the method used to calculate the noise identity. We could also define a noise equivalent resistance for a noise voltage as

$$R_n = \frac{\overline{V_A^2}}{4kTB} \quad (25)$$

The resistor  $R_n$  is not a physical resistor but can be used to simulate different portions of the noise equivalent circuit.

In a similar manner a mean-square current fluctuation can be represented in terms of an equivalent noise conductance  $G_n$ , which is defined by

$$G_n = \frac{\overline{I_A^2}}{4kTB} \quad (26)$$

and

$$G_u = \frac{\overline{I_u^2}}{4kTB} \quad (27)$$

for the case of the uncorrelated noise component. The input generator to the two-port has a similar contribution.

$$G_G = \frac{I_G^2}{4kTB} \quad (28)$$

with  $Y_G$  being the generator admittance and  $G_G$  being the real part. With the definition of  $F$  above, we can write

$$F = 1 + \left| \frac{I_A + Y_G V_A}{I_G} \right|^2 \quad (29)$$

The use of the voltage  $V_A$  and the current  $I_A$  has allowed us to combine all the effects of the internal noise sources. We can use the previously defined (22) correlation admittance,  $Y_{\text{cor}} = G_{\text{cor}} + jB_{\text{cor}}$ , to simplify (29). First, we determine the total noise current:

$$\overline{I_A^2} = 4kT(|Y_{\text{cor}}|^2 R_n + G_u)B \quad (30)$$

where  $R_n$  and  $G_u$  are defined in (25) and (26). The noise factor can now be determined.

$$F = 1 + \frac{G_u}{G_g} + \frac{R_n}{G_g} [(G_G + G_{\text{cor}})^2 + (B_G + B_{\text{cor}})^2] \quad (31)$$

$$F = 1 + \frac{R_u}{R_g} + \frac{G_n}{R_g} [(R_G + R_{\text{cor}})^2 + (X_G + X_{\text{cor}})^2] \quad (32)$$

The noise factor is a function of various elements, and the optimum impedance for the best noise figure can be determined by minimizing  $F$  with respect to generator reactance and resistance. This gives

$$R_{0n} = \sqrt{\frac{R_u}{G_n} + R_{\text{cor}}^2} \quad (33)$$

$$X_{0n} = -X_{\text{cor}} \quad (34)$$

and

$$F_{\text{min}} = 1 + 2G_n R_{\text{cor}} + 2\sqrt{R_u G_n + (G_n R_{\text{cor}})^2} \quad (35)$$

(To distinguish between optimum noise and optimum power, we have introduced the convention  $0n$  instead of the more familiar abbreviation *opt.*) At this point we see that the optimum condition for minimum noise figure is not a conjugate power match at the input port. We can explain this by recognizing that the noise source  $V_A$  and  $I_A$  represent all the two-port noise, not just the thermal noise of the input port. We should observe that the optimum generator susceptance,  $-X_{\text{cor}}$ , will minimize the noise contribution of the two noise generators.

In rearranging for conversion to  $S$  parameters, we write

$$F = F_{\text{min}} + \frac{g_n}{R_G} |Z_G - Z_{0n}|^2 \quad (36)$$

$$F = F_{\text{min}} + \frac{R_n}{G_G} |Y_G - Y_{0n}|^2 \quad (37)$$

From the definition of the reflection coefficient,

$$\Gamma_G = \frac{Y_0 - Y_G}{Y_0 + Y_G} \quad (38)$$

and with

$$g_G = \frac{G_G}{Y_0} \quad (39)$$

$$r_n = \frac{R_n}{Z_0} \quad (40)$$

the normalized equivalent noise resistance

$$F = F_{\min} + \frac{4r_n |\Gamma_G - \Gamma_{0n}|^2}{g_G (1 - |\Gamma|^2) |1 + \Gamma_{0n}|^2} \quad (41)$$

$$r_n = (F_{50} - F_{\min}) \frac{|1 + \Gamma_{0n}|^2}{4|\Gamma_{0n}|^2} \quad (42)$$

$$\Gamma_{0n} = \frac{Z_{0n} - Z_0}{Z_{0n} + Z_0} \quad (43)$$

The noise performance of any linear two-port can now be determined if the values of the four noise parameters,  $F_{\min}$ ,  $r_n = R_n/50$ , and  $\Gamma_{0n}$  are known. Figure 18 shows the noise factor of a high-frequency transistor as a function of  $B_g$  for  $G_g = \text{constant}$  and as a function of  $G_g$  for  $B_g = B_{opt}$ .

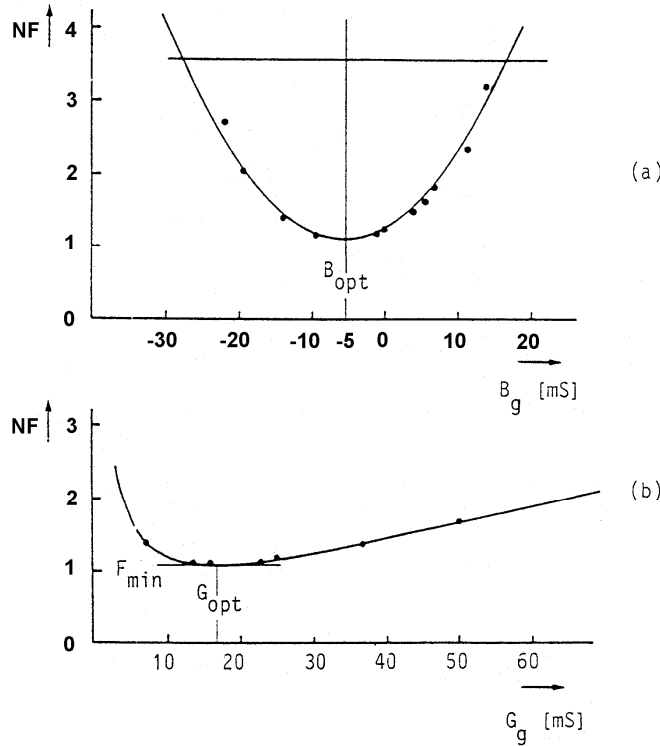


Figure 18: Noise factor in high-frequency BJTs for  $f = 600$  MHz: (a) as a function of  $B_g$  for  $G_g = \text{constant}$ ; (b), as a function of  $G_g$  for  $B_g = B_{opt}$ .

#### 4.2 Noise figure of cascaded networks.

In a system with many circuits connected in cascade (Figure 19), we must consider the contributions of the various circuits. In considering the equivalent noise resistor  $R_n$  in series with the input circuit.

$$F = \frac{R_G + R_n}{R_G} \quad (44)$$

$$F = 1 + \frac{R_n}{R_G} \quad (45)$$

The excess noise added by the circuit is  $R_n/R_G$ .

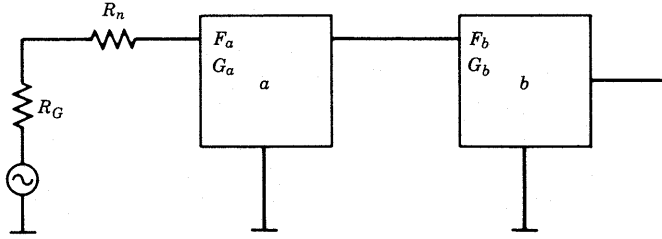


Figure 19: Cascaded noisy two-ports with the noise figures  $F_a$  and  $F_b$  and the gain figure  $G_a$  and  $G_b$ .

In considering two cascaded circuits  $a$  and  $b$ , by definition the available noise at the output of  $b$  is

$$N_{ab} = F_{ab} G_{ab} kTB \quad (46)$$

with  $B$  the equivalent noise bandwidth in which the noise is measured. The total available gain  $G$  is the product of the individual available gains, so

$$N_{ab} = F_{ab} G_a G_b kTB \quad (47)$$

The available noise from network  $a$  at the output of network  $b$  is

$$N_{a/b} = N_a G_b = F_a G_a G_b kTB \quad (48)$$

The available noise added by network  $b$  (its excess noise) is

$$N_{b/b} = (F_b - 1) G_b kTB \quad (49)$$

The total available noise  $N_{ab}$  is the sum of the available noise contributed by the two networks:

$$\begin{aligned} N_{ab} &= N_{a/b} + N_{b/b} = F_a G_a G_b kTB + (F_b - 1) G_b kTB \\ &= \left( F_a + \frac{F_b - 1}{G_a} \right) G_a G_b kTB \end{aligned} \quad (50)$$

$$F_{ab} = F_a + \frac{F_b - 1}{G_a} \quad (51)$$

For any number of circuits, this can be extended to be

$$F = F_1 + \frac{F_2 - 1}{G_1} + \frac{F_3 - 1}{G_1 G_2} + \frac{F_4 - 1}{G_1 G_2 G_3} + \dots \quad (52)$$

When considering a long chain of cascaded amplifiers, there will be a minimum noise figure achievable for this chain. This is a figure of merit and was proposed by Haus and Adler [6]. It is calculated by rearranging (52).

$$(F_{\text{tot}})_{\text{min}} = (F_{\text{min}} - 1) + \frac{F_{\text{min}} - 1}{G_A} + \frac{F_{\text{min}} - 1}{G_A^2} + \dots + 1 \quad (53)$$

where  $F_{\min}$  is the minimum noise figure for each stage and  $G_A$  is the available power gain of the identical stages.

Using

$$\frac{1}{1 - X} = 1 + X + X^2 + \dots \quad (54)$$

we find a quantity  $(F_{\text{tot}} - 1)$ , which is defined as the noise measure  $M$ . The minimum noise measure

$$(F_{\text{tot}})_{\min} - 1 = \frac{F_{\min} - 1}{1 - 1/G_A} = M_{\min} \quad (55)$$

refers to the noise of an infinite chain of optimally tuned, low-noise stages, so it represents a lower limit on the noise of an amplifier.

The minimum noise measure  $M_{\min}$  is an invariant parameter and is not affected by feedback. It is somewhat similar to a gain-bandwidth product, in its use as a system invariant. The minimum noise measure is achieved when the amplifier is tuned for the available power gain and  $\Gamma_G = \Gamma_{0n}$ , given by (43).

### 4.3 Noise correlation in linear two-ports using correlation matrices

Noise correlation matrices form a general technique for calculating noise in  $n$ -port networks. Haus and Adler have described the theory behind this technique [14]. In 1976, Hillbrand and Russer published equations and transformations that aid in supplying this method to two-port CAD [9].

This method is useful because it forms a base from which we can rigorously calculate the noise of linear two-ports combined in arbitrary ways. For many representations, the method of combining the noise parameters is as simple as that for combining the circuit element matrices. In addition, noise correlation matrices can be used to calculate the noise in linear frequency conversion circuits. The following is an introduction to this subject.

Linear, noisy two-ports can be modeled as a noise-free two-port with two additional noise sources. These noise sources must be chosen so that they add directly to the resulting vector of the representation, as shown in (56) and (57) and Figure 17.

$$\begin{bmatrix} I_1 \\ I_2 \end{bmatrix} = \begin{bmatrix} y_{11} & y_{12} \\ y_{21} & y_{22} \end{bmatrix} \begin{bmatrix} V_1 \\ V_2 \end{bmatrix} + \begin{bmatrix} i_1 \\ i_2 \end{bmatrix} \quad (56)$$

$$\begin{bmatrix} V_1 \\ V_2 \end{bmatrix} = \begin{bmatrix} z_{11} & z_{12} \\ z_{21} & z_{22} \end{bmatrix} \begin{bmatrix} I_1 \\ I_2 \end{bmatrix} + \begin{bmatrix} v_1 \\ v_2 \end{bmatrix} \quad (57)$$

where the  $i$  and  $v$  vectors indicate noise sources for the  $y$  and  $z$  representations, respectively. This two-port example can be extended to  $n$ -ports in a straightforward, obvious way.

Since the noise vector for any representation is a random variable, it is much more convenient to work with the noise correlation matrix. The correlation matrix gives us deterministic numbers to calculate with. The correlation matrix is formed by taking the mean value of the outer product of the noise vector. This is equivalent to multiplying the noise vector by its adjoint (complex conjugate transpose) and averaging the result:

$$\langle \bar{i} \bar{i}^+ \rangle = \begin{bmatrix} i_1 \\ i_2 \end{bmatrix} [i_1^* \quad i_2^*] = \begin{bmatrix} \langle i_1 i_1^* \rangle & \langle i_1 i_2^* \rangle \\ \langle i_1^* i_2 \rangle & \langle i_2 i_2^* \rangle \end{bmatrix} = [C_y] \quad (58)$$

where the angular brackets denote the average value.

Note that the diagonal terms are the "power" spectrum of each noise source and the off-diagonal terms are complex conjugates of each other and represent the cross "power" spectrums of the noise sources. "Power" is used because these magnitude-squared quantities are proportional to power.

To use these correlation matrices in circuit analysis, we must know how to combine them and how to convert them between various representations. An example using y matrices will illustrate the method for combining two-ports and their correlation matrices. Given two matrices y and y', when we parallel them we have the same port voltages, and the terminal currents add (Figure 20).

$$\begin{aligned} I_1 &= y_{11}V_1 + y_{12}V_2 + y'_{11}V_1 + y'_{12}V_2 + i_1 + i'_1 \\ I_2 &= y_{21}V_1 + y_{22}V_2 + y'_{21}V_1 + y'_{22}V_2 + i_2 + i'_2 \end{aligned} \quad (59)$$

or

$$\begin{bmatrix} I_1 \\ I_2 \end{bmatrix} = \begin{bmatrix} y_{11} + y'_{11} & y_{12} + y'_{12} \\ y_{21} + y'_{21} & y_{22} + y'_{22} \end{bmatrix} \begin{bmatrix} V_1 \\ V_2 \end{bmatrix} + \begin{bmatrix} i_1 + i'_1 \\ i_2 + i'_2 \end{bmatrix} \quad (60)$$

Here we can see that the noise current vectors add just as the y parameters add. Converting the new noise vector to a correlation matrix yields

$$\langle \bar{i}_{\text{new}} \bar{i}_{\text{new}}^+ \rangle = \left\langle \begin{bmatrix} i_1 + i'_1 \\ i_2 + i'_2 \end{bmatrix} [i_1^* + i_1'^* \quad i_2 i_2'^*] \right\rangle \quad (61)$$

$$= \begin{bmatrix} \langle i_1 i_1^* \rangle + \langle i_1' i_1'^* \rangle & \langle i_1 i_2^* \rangle + \langle i_1' i_2'^* \rangle \\ \langle i_2 i_1^* \rangle + \langle i_2' i_1'^* \rangle & \langle i_2 i_2^* \rangle + \langle i_2' i_2'^* \rangle \end{bmatrix} \quad (62)$$

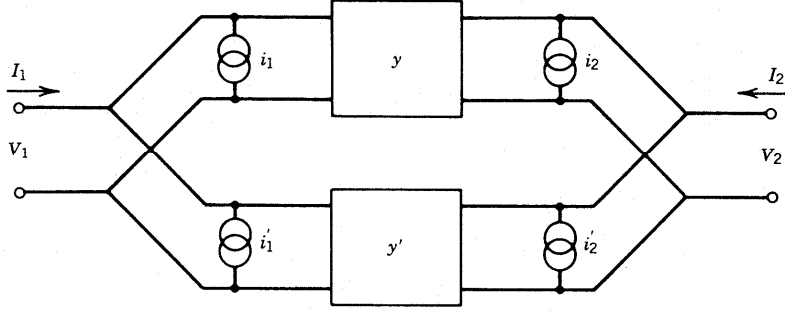


Figure 20: Parallel combination of two-ports using y parameters.

The noise sources from different two-ports must be uncorrelated, so there are no cross products of different two-ports. By inspection, (60) is just the addition of the correlation matrices for the individual two-ports, so

$$[C_{y_{\text{new}}}] = [C_y] + [C_{y'}] \quad (63)$$

The same holds true for \$g\$, \$h\$, and \$z\$ parameters, but \$ABCD\$ parameters have the more complicated form shown below. If

$$[A_{\text{new}}] = [A][A'] \quad (64)$$

then

$$[C_{A_{\text{new}}}] = [C_A] + [A][C_{A'}][A]^+ \quad (65)$$

The transformation of one representation to another is best illustrated by an example. Let us transform the correlation matrix for a \$Y\$ representation to a \$Z\$ representation. Starting with

$$\begin{bmatrix} I_1 \\ I_2 \end{bmatrix} = [Y] \begin{bmatrix} V_1 \\ V_2 \end{bmatrix} + \begin{bmatrix} i_1 \\ i_2 \end{bmatrix} \quad (66)$$

we can move the noise vector to the left side and invert \$y\$:

$$\begin{bmatrix} V_1 \\ V_2 \end{bmatrix} = [Y^{-1}] \begin{bmatrix} I_1 - i_1 \\ I_2 - i_2 \end{bmatrix} = [Y^{-1}] \begin{bmatrix} I_1 \\ I_2 \end{bmatrix} + [Y^{-1}] \begin{bmatrix} -i_1 \\ -i_2 \end{bmatrix} \quad (67)$$

Since \$(Y)^{-1} = (Z)\$, we have

$$\begin{bmatrix} V_1 \\ V_2 \end{bmatrix} = [Z] \begin{bmatrix} I_1 \\ I_2 \end{bmatrix} + [Z] \begin{bmatrix} -i_1 \\ -i_2 \end{bmatrix} \quad (68)$$

so

$$= [Z] \begin{bmatrix} -i_1 \\ -i_2 \end{bmatrix} = [T_{yz}] \begin{bmatrix} -i_1 \\ -i_2 \end{bmatrix} \quad (69)$$

where the signs of  $i_1$  and  $i_2$  are superfluous since they will cancel when the correlation matrix is formed. Here the transformation of the  $Y$  noise current vector to the  $Z$  noise voltage vector is done simply by multiplying by  $(Z)$ . Other transformations are shown in Table 1.

**Table 1: Noise Matrix  $T_{\alpha\beta}$  Transformation**

		Original Form ( $\alpha$ Form)					
		$Y$		$Z$		$A$	
Resulting Form ( $\beta$ Form)	$Y$	1	0	$y_{11}$	$y_{12}$	$-y_{11}$	1
		0	1	$y_{21}$	$y_{22}$	$-y_{21}$	0
	$Z$	$z_{11}$	$z_{12}$	1	0	1	$-z_{11}$
		$z_{21}$	$z_{22}$	0	1	0	$-z_{21}$
	$A$	0	$A_{12}$	1	$-A_{11}$	1	0
		1	$A_{22}$	0	$-A_{21}$	0	1

To form the noise correlation matrix, we gain from the mean of the outer product:

$$\langle vv^+ \rangle = \begin{bmatrix} \langle v_1 v_1^* \rangle & \langle v_1 v_2^* \rangle \\ \langle v_1^* v_2 \rangle & \langle v_2 v_2^* \rangle \end{bmatrix} = [Z] \left\langle \begin{bmatrix} i_1 \\ i_2 \end{bmatrix} [i_1^* \ i_2^*] \right\rangle [Z]^+ \quad (70)$$

or

$$[C_z] = [Z] [C_y] [Z]^+ \quad (71)$$

where

$$v^+ = [i_1^* \ i_2^*] [Z]^+ \quad (72)$$

This is called a congruence transformation. The key to all of these derivations is the construction of a correlation matrix from the noise vector, as shown in (60). These correlation matrices may easily be derived from the circuit matrices of passive circuits with only thermal noise sources. For example,

$$[C_z] = 2kT\Delta f \operatorname{Re}([Z]) \quad \text{and} \quad (73)$$

$$[C_y] = 2kT\Delta f \operatorname{Re}([Y]) \quad (74)$$

The  $2kT$  factor comes from the double-sided spectrum of thermal noise. The correlation matrix from the  $ABCD$  matrix may be related to the noise figure, as shown by Hillbrand and Russer [9]. We have

$$F = 1 + \frac{\bar{Y}[C_a]\bar{Y}^+}{2kT \operatorname{Re}(Y_G)} \quad (75)$$

where

$$\bar{Y} = \begin{bmatrix} Y_G \\ 1 \end{bmatrix}$$

Expressing the noise factor in terms of the correlation matrix, here is a complete formula:

$$F = 1 + \frac{C_{22}^A(f) + 2 \operatorname{Re}\{Y_g(f) C_{12}^A(f)\} + |Y_g(f)|^2 C_{11}^A(f)}{2 k T_0 \operatorname{Re}\{Y_g(f)\}} \quad (76)$$

Once we transform this in the  $Y$  parameter form, we obtain the following equation:

$$F(f) = F_{\min}(f) + \frac{R_n(f) |Y_{opt}(f) - Y_g(f)|^2}{\operatorname{Re}\{Y_g(f)\}} \quad (77)$$

It should be noted that all these values are frequency-dependent as expressed in this equation. The  $ABCD$  correlation matrix can be written in terms of the noise-figure parameters as (double-sided spectrum)

$$[C_a] = 2kT \begin{bmatrix} R_n & \frac{F_0 - 1}{2} - R_n Y_{0n}^* \\ \frac{F_0 - 1}{2} - R_n Y_{0n} & R_n |Y_{0n}|^2 \end{bmatrix} \quad (78)$$

The noise correlation matrix method forms an easy and rigorous technique for handling noise in networks. This technique allows us to calculate the total noise for complicated networks by combining the noise matrices of subcircuits. It should be remembered that although noise correlation matrices apply to  $n$ -port networks, noise-figure calculations apply only to pairs of ports. The parameters of the  $C_a$  matrix can be used to give the noise parameters:

$$Y_{0n} = \sqrt{\frac{C_{ii^*}}{C_{uu^*}} - \left[ \operatorname{Im}\left(\frac{C_{ui^*}}{C_{uu^*}}\right) \right]^2} + j \operatorname{Im}\left(\frac{C_{ui^*}}{C_{uu^*}}\right) \quad (79)$$

$$F_0 = 1 + \frac{C_{ui^*} + C_{uu^*} Y_{0n}^*}{kT} \quad (80)$$

$$R_n = C_{uu^*} \quad (81)$$

## 5. TRANSMISSION LINE MODELS AND OTHER MICROWAVE CONNECTING ELEMENTS

In order to decouple the transistor from the biasing, we use RF chokes and dc decoupling (bypass) capacitors. This is the technique we have already used in the previous examples, so one might ask the question, "What's new?" As frequency increases, these inductors are either not manufacturable or have such a low  $Q$  that their use becomes questionable. This is the point where one may introduce the so-called distributed elements.

Figure 21 shows the general RF amplifier circuit but resorting to distributed rather than lumped elements. The elements we are introducing now are part of any good, up-to-date CAD tool.

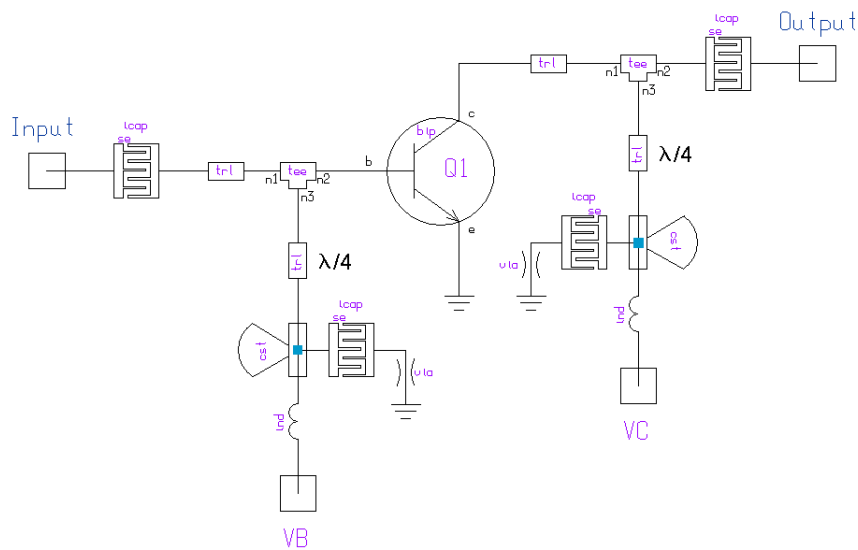


Figure 21: Simple BJT RF amplifier with distributed elements.

- Transmission Line

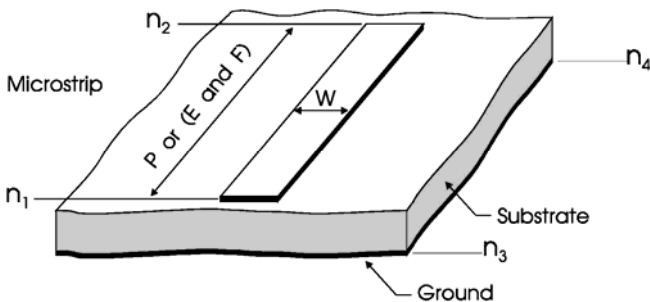


Figure 22: Transmission line in microstrip.

Any printed connection between two points on a circuit board is a transmission line (Figure 22). Its characteristic electrical impedance is a function of the square root of the dielectric constant ( $\epsilon_r$ ), the width, metallization, thickness and height above substrate of the line, and the loss tangent of the substrate. Since lines frequently have to be laid out in the form of curved connections or have a bend in their direction, we have to add

elements capable of describing the high-frequency consequences of such connections. Figures 23 and 24 show mitered and radial bend elements that perform this function.

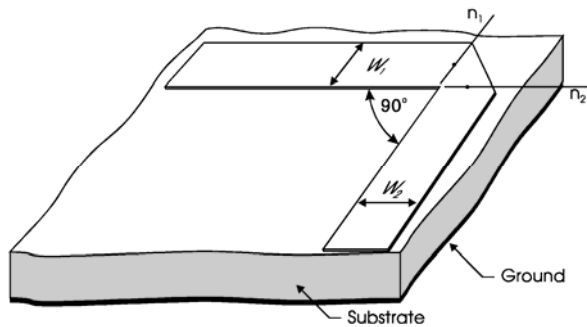


Figure 23: Mitered bend.

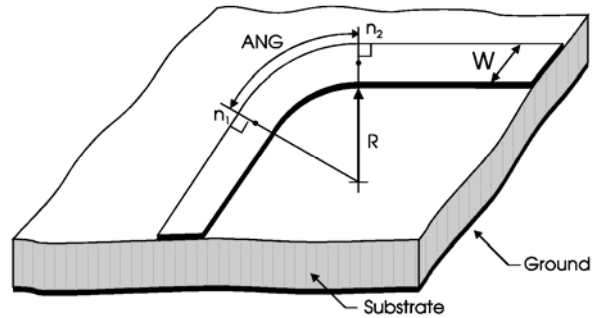


Figure 24: Radial bend.

- T, Cross, and Y junction

By the time a point like a collector or base, or its FET equivalent, spreads out into connecting with other elements, we need additional modeling capability to describe T connections, crossings, and Y junctions. Figures 25, 26, and 27 show the way in which these connections need to be modeled.

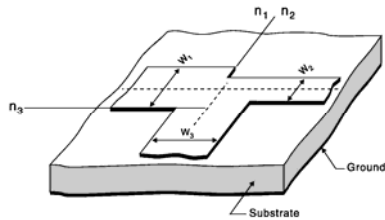


Figure 25: T junction.

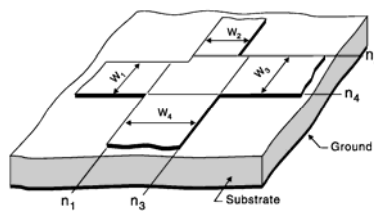


Figure 26: Cross.

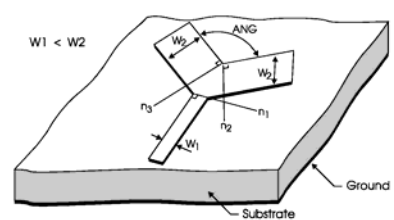


Figure 27: Y junction.

If the need exists the standard inductances must be replaced with a transmission line whose length is  $\lambda/8$  at the operating frequency. At higher frequencies, these transmission lines, however, then go into  $\lambda/4$  resonant mode and later become capacitive. This type of design makes it fairly narrowband. A way around this is the use of printed inductors, as shown in Figures 28 and 29.

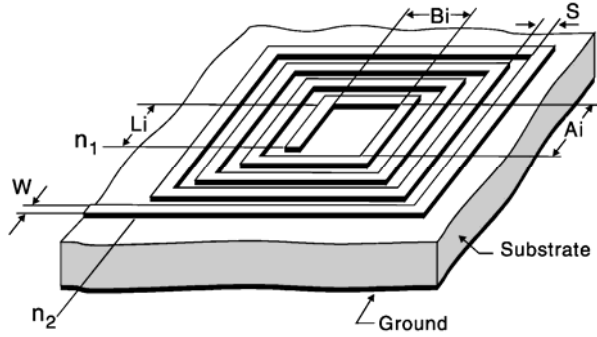


Figure 28: Rectangular inductor.

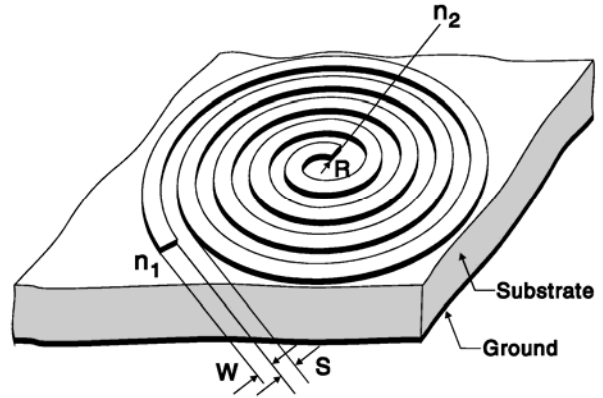


Figure 29: Spiral inductor.

These inductors have a self-resonant frequency similar to the transmission line mentioned above, but the safety margin is significantly higher.

Talking about printed inductors, a logical extension of this is the printed transmission-line-based transformer as shown in Figure 30. One can consider this as two interlaced rectangular inductors, and based on the substrate material, they are useful over a wide frequency range. Besides being used as a transformer, they can also be used to transit from unbalanced to balanced transmission provided that the difference in length from a connection point of view does not cause any problems (this is a layout issue).

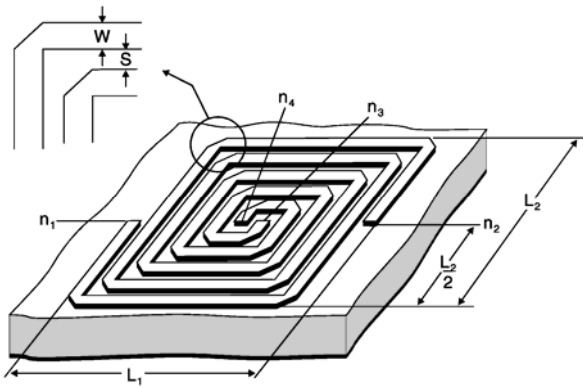


Figure 30: Transformer in microstrip.

A popular form of combining stages is the so-called Lange coupler (Figure 31) invented by the German Julius Lange. It is one of the major contributions in wideband applications.

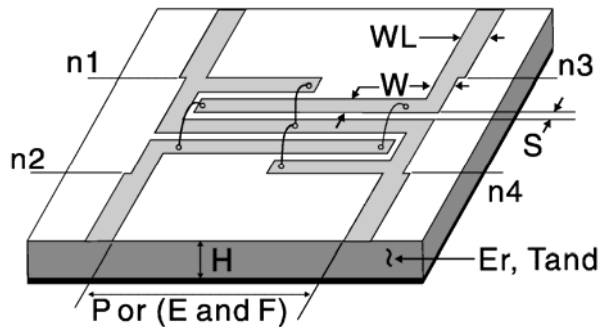


Figure 31: Four-strip Lange coupler.

The useful application of the Lange coupler probably starts at 4GHz. It consists of parallel transmission lines with the appropriate connections as shown. Lange couplers are typically built with four, six, and eight fingers. The Ansoft Serenade product has a Lange coupler synthesis program that can be used to gain more insight into this coupler's application. We assume that other modern software has similar capabilities.

Where meander-type of inductors are necessary a neat way to implement and simulate them is to use the multiple coupled line element (Figure 32) of the Serenade product, which both fast and accurately calculates the behavior of the meander, including self-resonances and losses. We made use of this arrangement in our previous examples.

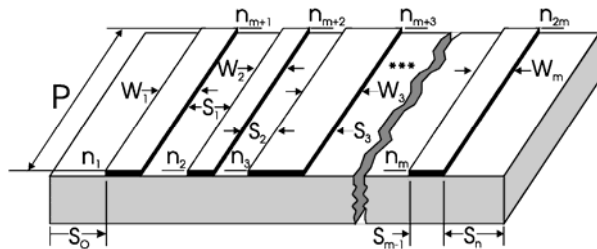


Figure 32: Multiple coupled lines element in microstrip.

- Interdigital Capacitors

The issue of tolerances of small capacitors already has been raised. The interdigital capacitor can be made on printed circuit board material as well as gallium arsenide, and if its dimensions are continuous with the transmission-line width does not cause any abrupt changes in the impedance. This type of capacitor permits to obtain very small values. By the way, an alternative to this is the use of transmission lines being  $3/8\lambda$ . We have learned above that a transmission line below its resonant frequency is inductive, goes into resonance, and then becomes capacitive. Again, bandwidth is also an issue. An interdigital capacitor consists of a number of parallel fingers as shown in Figure 33, and its capacitance can be varied by adjusting the number of fingers and their spacing. The advantage of the interdigital capacitor compared to discrete components is its low variation in value.

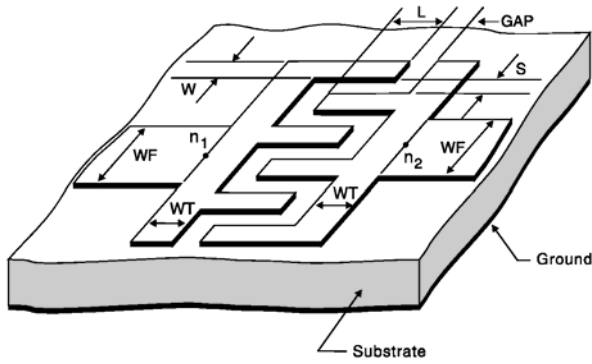


Figure 33: Interdigital capacitor.

- Radial Stubs

The radial stub (Figure 34) is not much different from a  $\lambda/4$  resonator, but its bandwidth is much greater than a simple transmission line. This is another way to ground the "cold" side of a transmission line or part of a circuit that needs to be grounded for RF. Of course, the interdigital capacitor comes in a version that is a combination of a capacitor and a via hole.

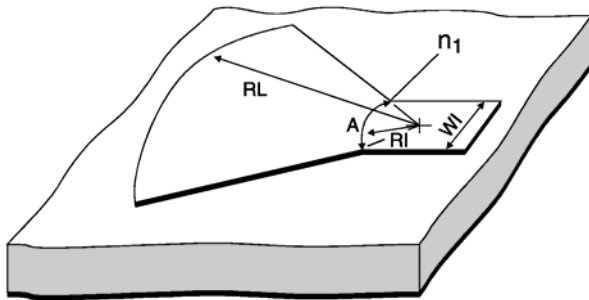


Figure 34: Radial stub.

- Via Holes

The "cold" end of the transmission line, being either considered an inductor or capacitor needs to be connected to a sufficiently large copper backplane. One very efficient way to do this, especially if there is not enough copper left on the top of the board, is the use of via holes (Figure 35). One could theoretically generate a via hole with a rivet, but most manufacturing processes don't allow this; the normal solution is to use plated-through holes left open. In the PC boards, via holes are typically cylindrical; on substrates like GaAs, they may be conical.

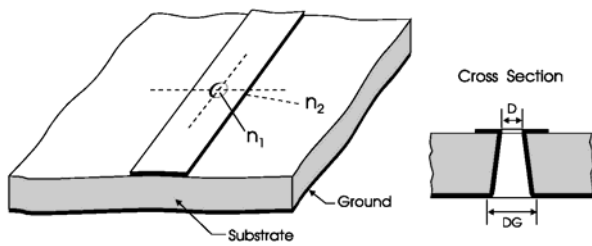


Figure 35: Via hole.

- Correction Elements

Although the behavior of actual circuits proceeds regardless of our ability to measure and describe it, we do not enjoy this luxury in simulating circuit behavior in software. In a simulator, effects that are insufficiently described will be inaccurately simulated. For instance, segments of high-impedance transmission line ( $120\Omega$ , for example) are frequently used for dc feeds and RF chokes. In predicting the effect of a transition from  $120\text{-}\Omega$  line to  $50\text{-}\Omega$  line, a simulator must be alerted to the discontinuity so it can do the necessary mathematical corrections to account for the impedance jump. To do this, a specific circuit element, the STEP (Figure 36), must be inserted between the  $120\text{-}\Omega$  and  $50\text{-}\Omega$  line elements in the simulation circuit file. In addition to substrate data, we characterize a STEP by providing the widths of its input and output lines. The element itself has no physical length.

A similar correction is necessary if a transmission line is used as a resonator or just "left open" at one end. Such a transmission line tends to radiate, and because of its high-impedance properties reacts differently as far as its electrical length is concerned. A zero-length one-port element, the OPEN (Figure 37), must be added to such a line for mathematically correct calculation.

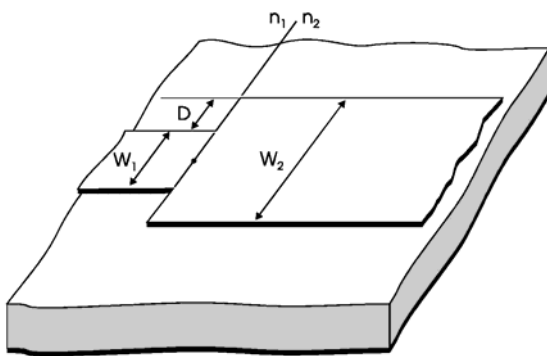


Figure 36: The STEP element tells the simulator to calculate the effects of joining transmission lines of differing characteristics.

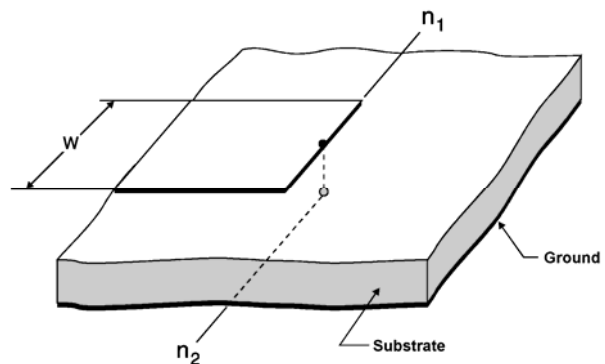


Figure 37: The OPEN element tells the simulator to calculate the effects of leaving the end of a transmission line unconnected.

We end this excursion into distributed elements here. Interested readers may want to obtain a CD containing the element library of their favorite CAD tools that combine capabilities in the microwave area with a full set of distributed circuit elements. It is most important to keep in mind that as frequency increases, we rapidly move into the area where we must consider all these distributed elements to achieve accurate simulations--even if doing so makes simulation a painful and time-consuming effort.

Finally, anyone who adventures in this area *must* obtain a foundry manual from the company that will build the integrated circuit or hybrid under design. There are basically two foundries, one applicable for MOS technology and one for GaAs. In the case of the bipolar transistor, the foundry service is not yet well-established. While we were able to interest one German company and one US company in generating a custom bipolar IC within the activities of this book, the only "open" foundry we know of for bipolar (actually HBT) technology is the one by TRW. As of

1999, this seems to be the leading company for BJT-related products, and many currently available ICs have been developed with this foundry service.

We mention the issue of foundries here again because each foundry has its own proprietary approach to modeling discontinuities. The availability of a foundry service somewhat eases the requirement that a designer be fully up to speed on the nuances of discontinuities, because a foundry's designer service will help customers account for all relevant parasitics or discontinuities in their designs. In addition, there are tables of  $S$  parameters provided by the vendor for standard cells of either capacitors, resistors, or inductors. The designer may then be forced to adjust the circuit so that it will work with a particular inductance value or value of another component within the resolution of the table that describes these elements. Information on the active part such as diodes and transistors is provided below and the details can be found in ref [10]

## 6. ACTIVE DEVICE MODELS

### 6.1 Typical SPICE parameters and sources

This Web site makes available a large number of needed time domain (SPICE) parameters:

[homepages.which.net/~paul.hills/Circuits/Spice/ModelIndex.html](http://homepages.which.net/~paul.hills/Circuits/Spice/ModelIndex.html)

Since we are about to evaluate bipolar microwave transistors, junction FETs, MOSFETs (model level 3), and GaAs FETs, here is a list of typical parameters for the devices we have used. These parameters can be obtained by a suitable program with the appropriate measurements. The BSIM model for MOSFETs, applicable for sub-micron technology transistors, requires an enormous level of parameter extraction and has not fully been validated for the LDMOS-type transistors currently favored for RF and microwave applications.

The meaning and significance of the various parameters is best explored in a book on SPICE or semiconductor physics [15,16,17].

#### Some Popular Devices

**Table 2: BFR193W BJT**

IS=2.738e-16	BF=125	NF=0.95341
VAF=24	IKF=0.26949	ISE=1.0627e-14
NE=1.935	BR=14.267	NR=1.4289
VAR=3.8742	IKR=0.037925	ISC=3.7409e-17
NC=0.94371	RB=15	IRB=0.00091763
RBM=1.8368	RE1=0.76534	RC2=0.11938
CJE=1.1824e-15	VJE=0.70276	MJE=0.48654
TF=1.8828e-11	XTF=0.69477	VTF=0.8
ITF=0.00096893	PTF=0	CJC=9.3503e-13
VJC=1.1828	MJC=0.30002	XCJC=0.053563
TR=1.0037e-09	VJS=0.75	MJS=0
XTB=0	EG=1.11	XTI=3
FCC=0.72063	LB=0.57e-9	LC=0.00e-9
LE=0.43e-9	CBCP=0.101E-12	CCEP=0.175E-12
CBEP=0.061e-12	VCMX=10V	

**Table 3: 2SK125 JFET**

```

IDSS= .5250E-01  VP0 = -.3111E+01  GAMA= -.1867E-01  E   = .1520E+01
KE   = -.3856E-03  SL   = .2818E-01  KG   = -.2398E+00  T   = .0000E+00
SS   = .7448E-04  IG0  = .2000E-14  AFAG= .3846E+02  IB0 = .1000E-04
AFAB= .3800E+02  VBC  = .3000E+02  R10  = .1711E+02  KR  = .0000E+00
C10  = .6609E-11  K1   = .1675E+01  C1S  = .6818E-33  CF0 = .7261E-11
KF   = .1156E+01  RG   = .5000E+00  RD   = .1542E+01  RS  = .1333E+01
LG   = .6098E-09  LD   = .5159E-08  LS   = .1482E-08  CDS = .4813E-16
CGE  = .1590E-11  CDE  = .3394E-26  CGSP= .8282E-13  CDSP= .4832E-12
ZGT  = .5000E+02  LGT  = .4712E-01  ZDT  = .5000E+02  LDT = .3998E-01
CGDP= .3653E-12  ZST  = .5000E+02  LST  = .1495E-01  CGDE= .3831E-12
CGSB= .3120E-13  CDSB= .5896E-12  VDMX=10

```

Note for junction FETs: The currently implemented model for junction FET is too primitive for serious RF applications. We have therefore taken the approach (liberty) to use the Materka parameter extraction approach for silicon junction FETs. This has resulted in unparalleled high quality parameters; in particular, the knee voltage behavior has significantly improved, as well as the overall frequency response.

**Table 4: GaAs MESFET**

```

IDSS= .1077E+00  VP0 = -.1800E+01  GAMA= -.5741E-01  E   = .1290E+01
KE   = -.1155E-01  SL   = .1652E+00  KG   = -.1782E+00  T   = .0000E+00
SS   = -.1208E-02  IG0  = .2130E-11  AFAG= .2740E+02  IB0 = .5680E-09
AFAB= .1826E+01  VBC  = .9000E+01  R10  = .8382E+01  KR  = .6359E+00
C10  = .5964E-12  K1   = .1296E+01  C1S  = .0000E+00  CF0 = .6110E-13
KF   = .9775E+00  RG   = .1996E+01  RD   = .1296E+01  RS  = .1234E+01
CDS  = .7852E-13  CDSD= .1000E-07  RDS  = .1581E+03  CGE = .1609E-12
CDE  = .8674E-13  VDMX=8

```

**Table 5: 1  $\mu\text{m}$   $\times$  750  $\mu\text{m}$  Level 3 LDMOS FET**

```

CBD = 0.863E-12  CGD0 = 166E-12  CGS0 = 246E-12  GAMA = 0.211
IS  = 6.53E-16  KAPA = 0.809    MJ  = 0.536    NSUB = 1E15
PB  = 0.71     PBSW = 0.71     PHI = 0.579    RD  = 39
RS  = 0.1     THET = 0.588   TOX = 4E-8     U0  = 835
VMAX = 3.38E5  VT0  = 2.78    XQC  = 0.41

```

## 7. NOISE MODELING

### Diode Noise Model.

The noise model for the diodes (Figure 38) consists of two contributions: the shot noise and the flicker noise. The shot noise is computed automatically and does not require any parameters. The flicker noise can be specified in two ways:

1. Using the enhanced SPICE noise model by specifying KF, AF, and FCP in the model\ parameter list (this option is usually sufficient for most applications).
2. Using bias-dependent flicker noise coefficients (specifying KF and AF at multiple bias points).

### Diode Noise Model Keywords

keyword	description	unit	default
<b>ID</b>	Required bias current for the data point	Ampere	
<b>KF</b>	Flicker noise coefficient		0.0
<b>AF</b>	Bias exponent of the flicker noise model		1.0
<b>FCP</b>	Frequency exponent of the flicker noise model		1.0
<b>FC</b>	Flicker noise corner frequency	Hz	

The noise generators in the diode noise model are the series parasitic resistance,  $R_s$ , and the intrinsic junction. The figure below illustrates the intrinsic junction noise generator. Let  $\Delta f$  be the bandwidth (usually normalized to 1 Hz). The intrinsic noise generator has a mean-square value of:

$$\langle i_{Dn}^2 \rangle = 2qI_D \Delta f + KF \frac{I_D^{AF}}{f^{FCP}} \Delta f \quad (82)$$

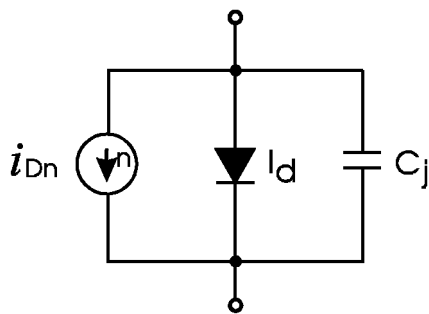


Figure 38: Equivalent noise circuit for a diode chip.

Notes on the Diode Noise Model:

1. Shot noise is always present unless the SN parameter is set to zero. Turning noise off is useful for comparing the total circuit noise that is generated by the nonlinear devices and that generated by the linear circuit components.

2. If the value of KF is specified as zero, then the flicker noise will not be contributed by the device and only shot noise is considered in the intrinsic model.
3. The corner frequency noise model uses the system noise floor to internally compute the flicker noise coefficient, KF. The system noise floor is computed by the program using the diode parameters and  $kT$ .
4. This noise model of course considers the actual operating temperature, which must be supplied to the model.

### **BJT Noise Model.**

The noise model for the Gummel-Poon BJT model consists of two contributions: shot noise and the flicker noise. The shot noise is computed automatically and does not require any parameters. The flicker noise can be specified in two ways:

1. Using the enhanced SPICE noise model by specifying KF, AF, and FCP in the model parameter list (this option is usually sufficient for most applications).
2. Using bias-dependent flicker noise coefficients (specifying KF and AF at multiple bias points).

*Option 1: Specifying the Bias-Independent Flicker Noise Coefficient.* This option involves the straightforward specification of KF, AF, and FCP that are constant with bias, as in the SPICE noise model. Notes on Option 1:

1. Shot noise is always present unless it is turned off. Turning noise off is useful for comparing the total circuit noise that is generated by the nonlinear devices and that generated by the linear circuit components.
2. If the value of KF is specified as zero, flicker noise will not be contributed by the device and only shot noise is considered in the intrinsic model.

*Option 2: Specifying The Bias-Dependent Flicker Noise Coefficient or Flicker Corner Frequency*

Option 2 allows a bias-dependent flicker noise coefficient (that is, KF and AF vary with the bias point).

*BJT Noise Model Keywords*

<b>keyword</b>	<b>description</b>	<b>unit</b>	<b>default</b>
<b>IB</b>	<b>Required</b> base bias current for the data point	ampere	
<b>VCE</b>	<b>Required</b> collector-emitter voltage for the data point	volt	
<b>VBS</b>	Base-substrate voltage required for LPNP type when four nodes are used.	volt	
<b>VCS</b>	Collector-substrate voltage required for NPN or PNP type when four nodes are used.	volt-	
<b>KF</b>	Flicker noise coefficient		0.0
<b>AF</b>	Bias exponent of the flicker noise model		1.0
<b>FCP</b>	Frequency exponent of the flicker noise model		1.0
<b>FC</b>	Flicker noise corner frequency	Hz	

*Notes on the BJT Noise Model:*

1. KF, AF, and FC can be specified as bias dependent. If only one set of noise data is specified, the corresponding bias point is not meaningful because all parameters are considered constant over all bias values. However, the bias point is needed for the program to identify the data as bipolar noise data.
2. The corner frequency noise model option uses the system noise floor to compute the flicker noise coefficient, KF. The system noise floor is computed by the program using the transistor parameters and  $kT$ .
3. This noise model of course considers the actual operating temperature, which must be supplied to the model.

Figure 33 shows the BJT noise model. Let  $\Delta f$  be the bandwidth (usually normalized to a 1-Hz bandwidth). The noise generators introduced in the intrinsic device are shown below, and have mean-square values of:

$$\langle i_{bn}^2 \rangle = 2qI_B \Delta f + KF \frac{I_B^{AF}}{f_{FCP}} \Delta f \quad (83)$$

$$\langle i_{cn}^2 \rangle = 2qI_C \Delta f \quad (84)$$

$$\langle i_{R_{bb}}^2 \rangle = \frac{4kT}{R_{bb}} \Delta f \quad (85)$$

$$\langle i_{R_{e1}}^2 \rangle = \frac{4kT}{R_{e1}} \Delta f \quad (86)$$

$$\langle i_{R_{c2}}^2 \rangle = \frac{4kT}{R_{c2}} \Delta f \quad (87)$$

$$I_B = \frac{I_{bf}}{BF} + I_{le} \quad (88)$$

$$I_C = I_{cf} - I_{cr} \quad (89)$$

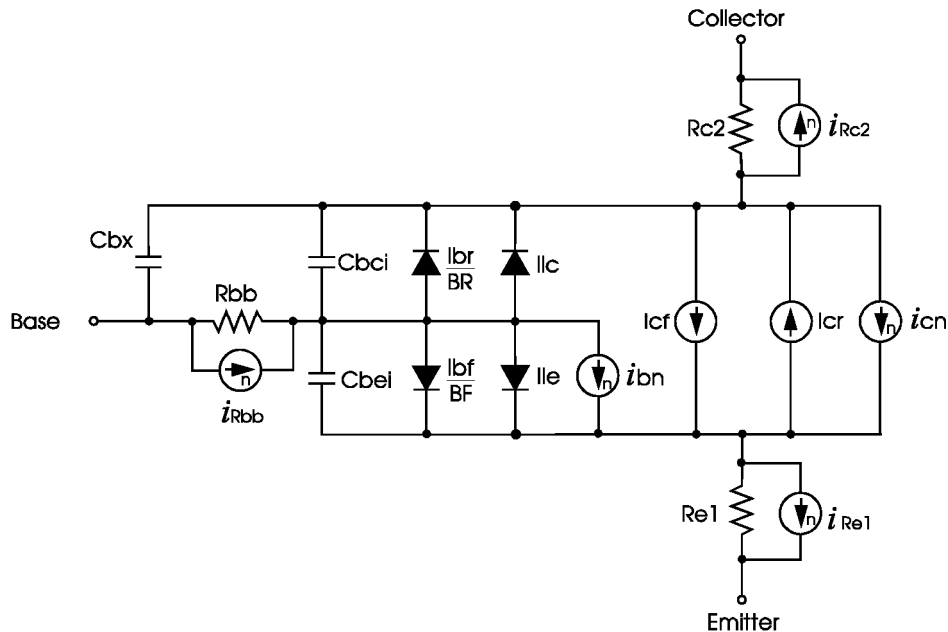


Figure 39: BJT noise model (not showing extrinsic parasitics). Current sources with  $n$  are noise sources.

### JFET and MESFET Noise Model.

The noise model for the FETs consists of two contributions: the shot noise and the flicker noise. There are two options to specify noise in the FET model:

1. Using the enhanced SPICE noise model by specifying KF, AF, and FCP in the model parameter list to determine the flicker noise (this option is usually sufficient for most applications). The shot noise will be automatically computed using the SPICE equation.
2. Using bias-dependent flicker noise coefficients through a reference in the DATA block (specifying KF and AF at multiple bias points) and specifying the four noise parameters (Fmin, MGopt, PGopt, and Rn) at multiple bias points.

*Option 1: Specifying the Enhanced SPICE Noise Model.* Option 1 is the straightforward specification of KF, AF, and FCP that are constant with bias, as in the SPICE noise model.

The drain noise model has the form:

$$\langle |I_{dn}|^2 \rangle = 4K_B T \frac{2g_m}{3} \Delta f + \text{KF} \frac{|I_D|^{\text{AF}}}{f^{\text{FCP}}} \Delta f \quad (90)$$

where the shot noise is derived from  $g_m$  and the flicker noise is proportional to KF and the drain channel current,  $I_D$ , and inversely proportional to frequency. The AF and FCP parameters tailor the flicker noise dependence on bias and frequency, respectively.

Notes on Option 1:

1. Shot noise is always present unless it is turned off. Turning noise off is useful for comparing the total circuit noise that is generated by the nonlinear devices and that generated by the linear circuit components.
2. If the value of KF is specified as zero, then flicker noise will not be contributed by the device and only shot noise is considered in the intrinsic model.

*(Option 2) Specifying The Bias-Dependent Flicker Noise Coefficient or Flicker Corner Frequency.* Option 2 allows the specification of the complex bias-dependent nature of the shot noise and flicker noise. At high frequencies, the equivalent noise sources are correlated (the SPICE noise model does not account for this correlation). The complete evaluation of the shot noise sources can be determined from the four noise parameters. Since these are functions of bias, they can be specified over the  $(V_{GS}, V_{DS})$  bias plane. Additionally, a bias-dependent flicker noise coefficient (that is, KF and AF vary with current) can be specified.

The MESFET noise model uses the four measured noise data ( $F_{min}$ ,  $\Gamma_{opt}$ , and  $R_n$ ) at one frequency and multiple arbitrary bias points. The program uses this data and the FET model parameters to de-embed the noise data to an intrinsic noise model. The intrinsic model is accurate at all frequencies, and therefore can predict the noise performance at all frequencies given data at just one frequency point. Built-in bias-dependent characteristics are used if multi-bias noise data is not provided.

*FET Noise Model Keywords*

<b>keyword</b>	<b>description</b>	<b>unit</b>	<b>default</b>
<b>FN</b>	Noise data measurement frequency	Hz	1.0 GHz
<b>VGS</b>	<b>Required</b> gate-source voltage for the data point	volt	
<b>VDS</b>	<b>Required</b> drain-source voltage for the data point	volt	
<b>FMIN</b>	<b>Required</b> minimum noise figure in dB at FN		
<b>MGO</b>	<b>Required</b> magnitude of optimum noise reflection coefficient at FN		
<b>PGO</b>	<b>Required</b> phase of optimum noise reflection coefficient at FN		
<b>RN</b>	<b>Required</b> normalized noise resistance at FN		
<b>KF</b>	Flicker noise coefficient		0.0
<b>AF</b>	Bias exponent of the flicker noise model		1.0
<b>FCP</b>	Frequency exponent of the flicker noise model		1.0
<b>FC</b>	Flicker noise corner frequency	Hz	

*Notes on the FET noise model:*

1. The corner frequency noise model option uses the system noise floor to compute the flicker noise coefficient, KF. The system noise floor is computed by the program using the transistor parameters and  $kT$ .
2. This noise model of course considers the actual operating temperature, which must be supplied to the model.

Noise in a MESFET is produced by sources intrinsic to the device. The same approach, but with different flicker corner frequencies, is highly applicable to JFETs and MOSFETs. For more detail as to simulation, see the Element library book for the active device portion of Ansoft's Serenade Design Environment product. The equivalent noisy circuit of an intrinsic FET is represented in Figure 40.

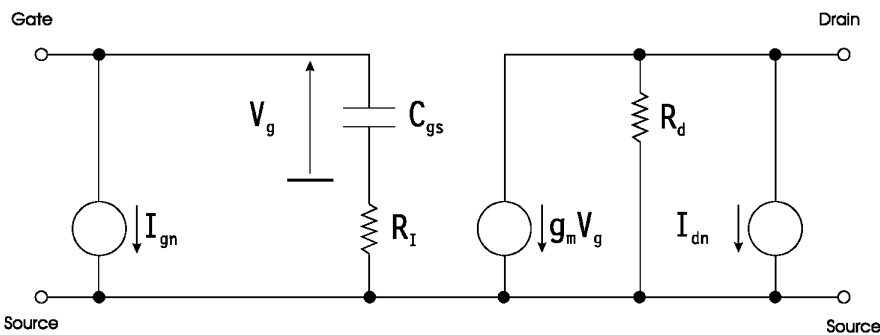


Figure 40: Equivalent noise circuit of an intrinsic FET device.

The intrinsic FET is internally represented as a noiseless nonlinear two-port with one equivalent noise current connected across the gate-source terminal, and one across the drain-source terminal. The correlations of the gate and drain noise current sources are:

$$\left\langle |I_{gn}|^2 \right\rangle = 4K_B T \Delta f \frac{\omega^2 C_{gs}^2}{g_m} R \quad (91)$$

$$\left\langle |I_{dn}|^2 \right\rangle = 4K_B T \Delta f g_m P \quad (92)$$

$$\left\langle I_{gn} I_{dn}^* \right\rangle = 4K_B T \Delta f j \omega C_{gs} \sqrt{PR} C \quad (93)$$

The correlation matrix of the noise current sources is

$$C_{dc}(\omega) = \frac{2}{\pi} K_B T d \omega \begin{bmatrix} \frac{\omega^2 C_{gs}^2}{g_m} R & -j \omega C_{gs} \sqrt{PR} C \\ j \omega C_{gs} \sqrt{PR} C & g_m P \end{bmatrix} \quad (94)$$

The gate and drain noise parameters  $R$  and  $P$  and the correlation coefficient  $C$  are related to the physical noise sources acting in the channel and are functions of the device structure and bias noise parameters. By defining measured noise parameters,  $F_{min}$ ,  $R_n$  and  $\Gamma_{opt}$ , and using a noise-de-embedding procedure, the parameters  $R$ ,  $P$ , and  $C$  and the intrinsic noise correlation matrix of a FET device as functions of device bias are determined by the program.

In addition to the noise sources shown above, the flicker ( $1/f$ ) noise can also be modeled by means of a noise current source connected in parallel with the intrinsic drain port. The flicker noise component in a narrow band,  $\Delta f$ , is expressed in the form

$$\left\langle |I_f|^2 \right\rangle = Q \Delta f \frac{|I_D|^{AF}}{f^{FCP}} \quad (95)$$

where  $I_D$  is the instantaneous value of the channel current, and  $Q$ ,  $AF$ , and  $FCP$  are empirical parameters. In most practical cases,  $AF$  and  $FCP$  are directly obtained from measurements (typically,  $AF = 2$  and  $FCP = 1$ ), while  $Q$  is not. In Ansoft's Serenade Design Environment,  $Q$  is either provided directly using  $KF$  or is computed by providing the flicker corner frequency ( $FC$ ).  $FC$  is the frequency at which the flicker noise equals the shot/diffusion noise. The corner frequency is defined by the equation

$$Q \frac{|I_D|^{AF}}{f_C^{FCP}} = g_m P \quad (96)$$

Given the corner frequency  $FC$  and the measurement bias point  $V_{gs}$  and  $V_{ds}$ , the program automatically computes  $I_D$ ,  $g_m$ , and  $P$ , and finally  $Q$ .

More information on FET noise modeling can be found in [18, 19, 20, 21, 22, 23 and 24].

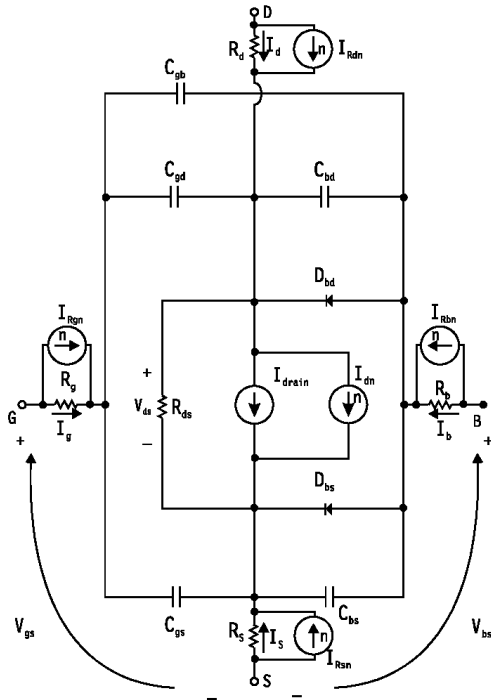


Figure 41: Equivalent noise circuit of an intrinsic MOSFET device.

### MOSFET Noise Model.

The MOSFET noise model (Figure 41) consists of two contributions: the shot noise and the flicker noise. The shot noise is computed automatically and does not require any parameters. It can be turned off by specifying  $SN = 0$ . The flicker noise can be specified in two ways:

1. Using the enhanced SPICE noise model by specifying KF, AF, and FCP in the model parameter list (this option is usually sufficient for most applications).
2. Using bias-dependent flicker noise coefficients through a reference (specifying KF and AF at multiple bias points).

#### *(Option 1) Specifying the Enhanced SPICE Noise Model*

Option 1 is the straightforward specification of KF, AF, and FCP that are constant with bias, as in the SPICE noise model (the flicker noise is considered bias dependent).

#### *Notes on the MOSFET Noise Model:*

1. Shot noise is always present unless the SN parameter is set to zero. Turning noise off is useful for comparing the total circuit noise that is generated by the nonlinear devices and that generated by the linear circuit components.

2. If the value of KF is specified as zero, then the flicker noise will not be contributed by the device and only shot noise is considered in the intrinsic model.

*(Option 2) Specifying The Bias-Dependent Flicker Noise Coefficient or Flicker Corner Frequency.*

Option 2 allows a bias-dependent flicker noise coefficient (that is, KF and AF varies with drain current). The MOSFET noise model data is given and referenced by a model parameter.

*Noise Model Keywords*

<b>keyword</b>	<b>description</b>	<b>unit</b>	<b>default</b>
<b>VGS</b>	<i>Required</i> gate-source bias for the data point	volt	
<b>VDS</b>	<i>Required</i> drain-source for the data point	volt	
<b>VBS</b>	<i>Required</i> drain-bulk for the data point	volt	
<b>KF</b>	Flicker noise coefficient		1.0E-13
<b>AF</b>	Bias exponent of the flicker noise model		2.0
<b>FCP</b>	Frequency exponent of the flicker noise model		1.0
<b>FC</b>	Flicker noise corner frequency	Hz	

*Notes on the MOSFET Noise Model:*

1. KF, AF, and FC can be specified as bias dependent. If only one set of noise data is specified, the corresponding bias point is not meaningful because all parameters are considered constant over all bias values. However, the bias point is needed for the program to identify the data as MOSFET noise data.

2. The corner frequency noise model option uses the system noise floor to compute the flicker noise coefficient, KF. The system noise floor is computed by the program using the transistor parameters and  $kT$ .

3. This noise model of course considers the actual operating temperature, which must be supplied to the model.

Let  $\Delta f$  be the bandwidth (normalized to 1 Hz). The noise generators introduced in the intrinsic device are shown below, and have mean-square values of:

$$\langle i_{dn}^2 \rangle = \frac{8kTg_m}{3} \Delta f + \text{KF} \frac{I_D^{\text{AF}}}{f^{\text{FCP}}} \Delta f$$

$$\langle i_{Rgn}^2 \rangle = 4 \frac{kT}{R_g} \Delta f$$

$$\langle i_{Rdn}^2 \rangle = 4 \frac{kT}{R_d} \Delta f$$

$$\langle i_{Rsn}^2 \rangle = 4 \frac{kT}{R_s} \Delta f$$

$$\langle i_{Rbn}^2 \rangle = 4 \frac{kT}{R_b} \Delta f$$

(97)

We include this MOSFET noise model (used for quite awhile) for completeness. At the moment, we do not know which MOSFET noise model the industry will settle on in the future.

Modern CAD tools, such as Ansoft's Serenade product, use these models allowing to generate quite accurate noise data based on a good linear equivalent model. Internally it uses the noise-correlation-matrix method (first introduced by Russer).

## 8. APPLICATIONS AND EXAMPLES

### Application 1

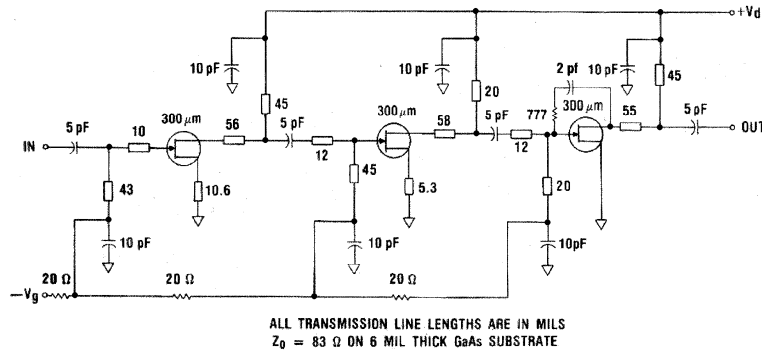


Figure 42: Schematic of the X-band GaAs monolithic low-noise amplifier (Texas Instruments EG8021).

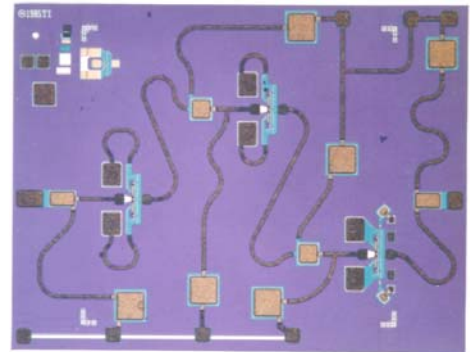


Figure 43: Photograph of the EG8021 monolithic amplifier chip. The area pictured is 0.09 inch by 0.12 inch in size.

Schematic of the X-band GaAs monolithic low-noise amplifier (Texas Instruments EG8021) (Figure 42) and its layout (Figure 43) are shown as example to rigorous modeling. The round transmission lines were chosen to reduce radiation and are beyond the analysis capacity of known simulators. It took a set of new models to be developed to accomplish this. For reasons of linearity, all three stages operate in Class A. This circuit was developed with some of the early devices and two test simulations were done. The first was the linear equivalent circuit of the transistors (total linear analysis) and then the non-linear time domain parameters were used, to validate their accuracy. Both approaches gave really good and similar answers. Compared to the measurements, the linear FET model gave a slightly closer answer, indicating that the non-linear model was not (correctly) optimized. This is a general phenomenon with non-linear models

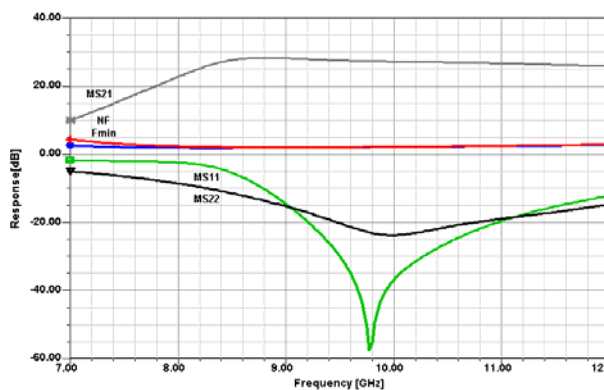


Figure 44: Simulated  $F_{min}$ , noise figure,  $S_{11}$ ,  $S_{21}$ , and  $S_{22}$  responses for the three-stage GaAsFET amplifier using the TI linear FET model. The values at 10 GHz are:  $F_{min}$ , 2.20 dB; NF, 2.21 dB;  $S_{11}$ , -36.8 dB;  $S_{21}$ , 27.2 dB; and  $S_{22}$ , -23.7 dB.

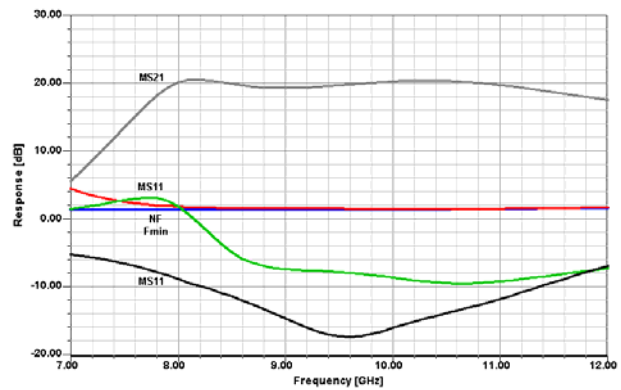


Figure 45: Simulated  $F_{min}$ , noise figure,  $S_{11}$ ,  $S_{21}$ , and  $S_{22}$  responses for the three-stage GaAsFET amplifier using the nonlinear FET model. The values at 10 GHz are:  $F_{min}$ , 1.53 dB; NF, 1.65 dB;  $S_{11}$ , -8.5 dB;  $S_{21}$ , 20.3 dB; and  $S_{22}$ , -15.9 dB.

## Application 2

In cooperation with Motorola, we also analyzed an 800-MHz VCO. In this case, we also did the parameter extraction for the Motorola transistor. Figure 5-46 shows the circuit, a Colpitts oscillator that uses RF feedback in the form of a 15- $\Omega$  resistor and a capacitive voltage divider consisting of 1 pF between the BJT's base and the feedback resistor, and 1 pF between the feedback resistor and common. Also, the tuned circuit is loosely coupled to this part of the transistor circuit. Figure 5-47 shows a comparison between predicted and measured phase noise for this oscillator.

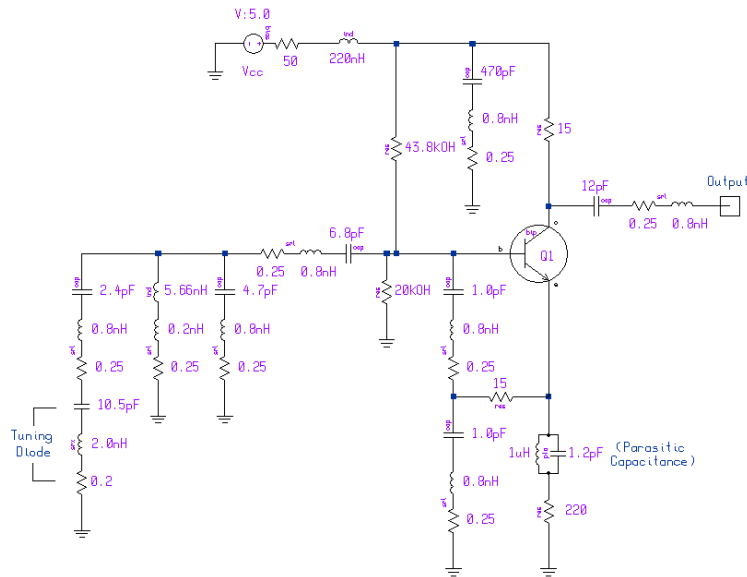


Figure 46: Colpitts oscillator for 800MHz with lumped elements modeled by their real values.

Figure 46 shows a Colpitts oscillator that uses RF negative feedback between the emitter and capacitive voltage divider. To be realistic, we have also used real components rather than ideal ones. The suppliers for the capacitors and inductors provide some typical values for the parasitics. The major changes are 0.8nH and 0.25 $\Omega$  in series with the capacitors. The same thing applies for the main inductance, which has a parasitic connection inductance of 0.2nH in series with a 0.25 $\Omega$  resistance. These types of parasitics are valid for a fairly large range of components assembled in surface-mount applications. Most engineers model the circuit only by assuming lossy devices, and not adding these important parasitics. One of the side-effects we have noticed is that the output power is more realistic and, needless to say, the simulated phase noise agrees quite well with measured data. This circuit can also serve as an example for modeling amplifiers and mixers using surface-mount components.

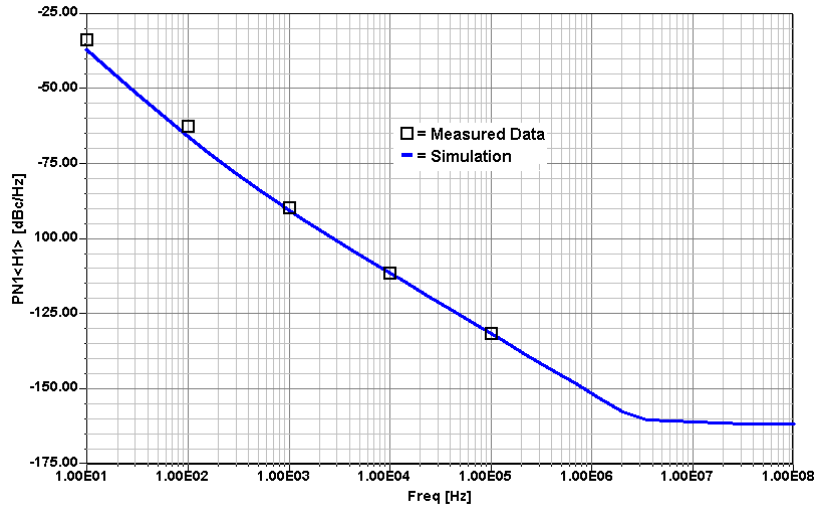


Figure 47: Comparison between predicted and measured phase noise for the oscillator shown in Figure 46.

## Bibliography and References

1. [bwrc.eecs.berkeley.edu/Classes/icbook/SPICE/](http://bwrc.eecs.berkeley.edu/Classes/icbook/SPICE/)
2. Transient Analysis of Microwave Oscillators by Krylov-Subspace Harmonic Balance
3. [www2.dac.com/App\\_Content/files/2009\\_Best\\_Paper\\_23.2.pdf](http://www2.dac.com/App_Content/files/2009_Best_Paper_23.2.pdf)
4. [en.wikipedia.org/wiki/Krylov\\_subspace](http://en.wikipedia.org/wiki/Krylov_subspace)
5. Carl T. A. Johnk, *Engineering Electromagnetic Fields and Waves*, New York: John Wiley & Sons, Inc. New York, NY, 1975, Chapter 5.
6. Robert Schetgen, ed., *The ARRL Handbook for Radio Amateurs*, 1995 edition, Newington: American Radio Relay League, 1995, chapters 6 and 24.
7. Jack Smith, *Modern Communication Circuits*, second ed. (New York: McGraw-Hill, 1997, ISBN 0-07-059283-7), pp. 93-99.
8. S. M. Perlow, "Third-Order Distortion in Amplifiers and Mixers," *RCA Review*, June 1976, pp. 234-265.
9. Edward C. Jordan, ed., *Reference Data for Engineers*, 7th Edition (Indianapolis: Howard W. Sams & Co, Inc, 1985, ISBN 0-672-21563-2), pp. 12-33 to 12-35.
10. U.L. Rohde and D. Newkirk, *RF/Microwave circuit design for wireless applications*, Wiley, NY 2000
11. Ulrich L. Rohde, Anthony M. Pavio, and Robert A. Pucel, "Accurate Noise Simulation of Microwave Amplifiers Using CAD," *Microwave Journal*, Vol. 31, No. 12, pp 130-141, December 1988.]
12. H. Rothe and W. Dhalke, "Theory of Noisy Fourpoles," *Proceedings of the IRE*, Vol. 44, June 1956, pp. 811-818.
13. "Representation of Noise in Linear Twoports," *Proceedings of the IRE*, Vol. 48, January 1960, pp. 69-74.
14. H. A. Haus and R. B. Adler, *Circuit Theory of Linear Noisy Networks*, Cambridge, Mass., MIT Press, 1959, and New York, Wiley, 1959.
15. Chris Bowick, *RF Circuit Design* (Indianapolis: Howard F. Sams & Co, 1982).
16. Adel S. Sedra and Kenneth C. Smith, *Microelectronic Circuits* (Chicago: Saunders College Publishing, 1991).
17. Paul R. Gray and Robert G. Meyer, *Analysis and Design of Analog Integrated Circuits*, second ed. (New York: John Wiley & Sons, Inc., 1984).
18. S. H. Lee, A. K. Wong, M. G. Wong, *A Current-Combiner Circuit for Better Mixer Conversion Gain*, Philips Semiconductors applications document.
19. F. M. Fano, "Theoretical Limitations in the Broadband Matching Arbitrary Impedances," *J. Franklin Institute*, Vol. 249, 1950, pp 57-85 and 139-155.
20. Ravender Goyal, ed., *High-Frequency Analog Integrated-Circuit Design* (New York: John Wiley & Sons, 1995, ISBN 0-471-53043--3), Chapter 6, Wideband Amplifiers.
21. Stefan Georgi and Ulrich L. Rohde, "A Novel Approach to Voltage Controlled Tuned Filters Using CAD Validation," *Microwave Engineering Europe*, October 1997, pp. 35-42.
22. *Analog/Interface ICs Device Data*, Vol. II, Q4/96, DL128, Rev 6, Motorola, Inc., MC13158 Wideband FM IF Subsystem specifications, pp 8-308-8-329.

23. E. J. Wilkinson, "An  $N$ -Way Power Divider," *IRE Trans. Microwave Theory Tech.*, Vol. MTT-8, January 1960, p 116.
24. Motorola Application Note AN-282A, *Systemizing RF Power Amplifier Design*.

## Appendix 1 - Krylov-subspace

In linear algebra, the order- $r$  **Krylov subspace** generated by an  $n$ -by- $n$  matrix  $A$  and a vector  $b$  of dimension  $n$  is the linear subspace spanned by the images of  $b$  under the first  $r$  powers of  $A$  (starting from  $A^0 = I$ ), that is,

$$\mathcal{K}_r(A, b) = \text{span} \{b, Ab, A^2b, \dots, A^{r-1}b\}.$$

It is named after Russian applied mathematician and naval engineer Alexei Krylov, who published a paper on this issue in 1931.

Modern iterative methods for finding one (or a few) eigenvalues of large sparse matrices or solving large systems of linear equations avoid matrix-matrix operations, but rather multiply vectors by the matrix and work with the resulting vectors. Starting with a vector,  $b$ , one computes  $Ab$ , then one multiplies that vector by  $A$  to find  $A^2b$  and so on. All algorithms that work this way are referred to as Krylov subspace methods; they are among the most successful methods currently available in numerical linear algebra.

Because the vectors tend very quickly to become almost linearly dependent, methods relying on Krylov subspace frequently involve some orthogonalization scheme, such as Lanczos iteration for Hermitian matrices or Arnoldi iteration for more general matrices.

The best known Krylov subspace methods are the Arnoldi, Lanczos, Conjugate gradient, GMRES (generalized minimum residual), BiCGSTAB (biconjugate gradient stabilized), QMR (quasi minimal residual), TFQMR (transpose-free QMR), and MINRES (minimal residual) methods.